IEEE Access
Multidisciplinary ⋮ Rapid Review ⋮ Open Access Journal

Received 24 February 2023, accepted 16 March 2023, date of publication 20 April 2023, date of current version 11 May 2023.

Digital Object Identifier 10.1109/ACCESS.2023.3268702

RESEARCH ARTICLE

Filter-Based Fault Detection and Isolation in Distributed Parameter Systems Modeled by Parabolic Partial Differential Equations

HASAN FERDOWSI[1], (Member, IEEE), JIA CAI[2], AND SARANGAPANI JAGANNATHAN[3], (Fellow, IEEE)

[1]Department of Electrical Engineering, Northern Illinois University, DeKalb, IL 60115, USA
[2]Microsoft Corporation, Redmond, WA 98052, USA
[3]Department of Electrical and Computer Engineering, Missouri University of Science and Technology, Rolla, MO 65401, USA

Corresponding author: Hasan Ferdowsi (hferdowsi@niu.edu)

ABSTRACT This paper covers model-based fault detection and isolation for linear and nonlinear distributed parameter systems (DPS). The first part mainly deals with actuator, sensor and state fault detection and isolation for a class of DPS represented by a set of coupled linear partial differential equations (PDE). A filter based observer is designed based on the linear PDE representation using which a detection residual is generated. A fault is detected when the magnitude of the detection residual exceeds a detection threshold. Upon detection, several isolation estimators are designed using filters whose output residuals are compared with predefined isolation thresholds. A fault on a linear DPS is declared to be of certain type if the corresponding isolation estimator output residual is below its isolation threshold while the other fault isolation estimator output residual is above its threshold. Next, the fault location is determined when a state fault is identified. The second part of this paper focuses on fault detection and isolation of nonlinear DPS by using a Luenberger type observer. Here fault isolation framework is introduced to isolate actuator, sensor and state faults with isolability condition by using additional boundary measurements and without filters. Finally, the effectiveness of the proposed fault detection and isolation schemes for both linear and nonlinear DPS are demonstrated through simulation.

INDEX TERMS Fault detection, fault isolation, distributed parameter systems, partial differential equations.

I. INTRODUCTION

In order to increase system availability and reliability, fault diagnosis has drawn significant attention in the area of modern control systems. Usually fault diagnosis consists of [1] (a) detection- to indicate the presence of a fault; (b) isolation- to determine the root cause and location of a fault; and (c) identification- to estimate the magnitude of a fault function. Fault isolation is a crucial step in fault diagnosis.

A variety of fault diagnosis approaches have been studied in the past two decades and between them, model-based methods [2] have found appealing since significant amount of healthy and faulty data is no longer required. Model-based fault detection and isolation methods have been developed for lumped parameter systems (LPS) represented by ordinary differential equations (ODEs) by using adaptive observer [3] sliding mode design [4] and fuzzy observers [5] fuzzy pole placement [6], and adaptive approximation [7]. Moreover, fault tolerant control for lumped parameter systems has been extensively studied, for example robust adaptive fault-tolerant consensus control [8] and fault-tolerant fuzzy formation control [9]. Despite the comprehensive effort, they [3], [4], [5], [6], [7], [8], [9] are only applicable for LPS.

However, many systems including heat transfer (for example thermal power plants and internal combustion engines), fluid flow (like oil pipelines and water treatment systems), and chemical processes (like chemical reactors and fuel cells) are characterized as distributed parameter systems (DPS) or infinite dimensional systems. Because of their

The associate editor coordinating the review of this manuscript and approving it for publication was Lei Shu.

distributed nature, the ODE representation cannot describe the DPS behavior [10] and they are usually modeled by partial differential equations (PDEs). Fault diagnosis of DPS is more complicated and challenging when compared to LPS since the system parameters are defined over a continuous range of both time and space [11].

In the early efforts, the DPS is approximated by finite dimensional ODE using Gelenkin's method [12] by assuming that the DPS is dominated by finite dimensional system with slow eigenvalues [13]. Subsequently, several articles appeared in the literature including an actuator failure detection method for DPS by identifying the actuator input [14]. An adaptive observer is developed in [15] to monitor the distributed parameter system and to provide information for the diagnosis of actuator faults. A geometric fault diagnosis approach, on the other hand, is introduced in [16] by approximating the PDE representation with a finite dimensional ODE. The authors of [17] use semidiscretization to transform the PDE model to a set of ODEs and then utilize Kalman filter and statistical decision making to diagnose faults. Fault detection and isolation of DPS with parabolic PDE models is investigated in [18] and [19] based on deriving a finite-dimensional ODE model via the Galerkin method. Despite these attractive results [14], [15], [16], [17], [18], [19], the fault detection and isolation of DPS based on approximated finite dimensional ODE can lead to an inaccurate model description and thus can result in false or missed alarms due to incorrect isolation.

Motivated by the model reduction concerns, authors investigated fault detection of DPS directly based on PDE representation of the system in [20], [21], and [22], unlike [14], [15], [16], [17], [18], [19]. While [20], [21] focus on fault diagnosis in linear DPS, [22] focuses on actuator and sensor fault detection and failure prediction in nonlinear DPS. Authors used an infinite dimensional adaptive observer to detect faults in [20]. To monitor system behavior, a detection residual signal, which is defined as the difference between the actual and estimated output of the observer, was generated. In the absence of a fault, this detection residual remains below a predefined detection threshold. A fault acts as an unwanted input to the detection residual dynamics and increasing it. A fault is declared active when this residual crosses the detection threshold. However, [20], [21] only consider linear PDE models and [22] is only on fault detection. Moreover, detectability condition for state faults and fault isolation is not covered in [20], [21], and [22].

Therefore, this paper extends the fault detection and prediction framework from [20], [21], and [22] to fault isolation by utilizing the PDE representation of linear DPS. First, the detectability condition of state faults is introduced. Upon detection by using the detection observer from [20], actuator and sensor fault isolation estimators are developed to identify the fault type when the output residual of the corresponding fault isolation estimator is below a predefined isolation threshold while the output residual of the other fault isolation estimator is above its threshold. In the event that the fault type is not an actuator and sensor, several state fault estimators located over the space are introduced to help determine the location of the state fault by using a second output measurement-spatial average over the sensed region. Several state fault isolation estimator residuals at different locations are derived and the one that is the minimum among them will determine the location of a potential state fault. Next, the magnitude of the fault parameter vector is estimated upon fault identification for all the fault types.

In the case of a nonlinear DPS, a Luenberger type observer from [23] is used for fault detection in the presence of bounded disturbances. For nonlinear DPS, due to lack of fault filters, isolation estimators cannot be derived and additional measurements are needed for fault isolation. By using additional measurements at the boundary condition and estimated output of the detection observer, an actuator/sensor isolation residual is generated. It will be shown that in the presence of an actuator or sensor fault, the corresponding isolation estimator output residual should exceed its corresponding isolation threshold, respectively while the other residual stays within its isolation threshold. To the contrary, when both sensor and actuator fault isolation estimator output residuals stay within their corresponding isolation thresholds, a state fault is considered to have occurred. Next, the isolability conditions are introduced to define the class of faults which can be isolated using the proposed scheme.

Note that the isolation framework for nonlinear DPS is different from linear DPS due to lack of filters in the case of nonlinear DPS. This weakness is overcome by using additional boundary measurements. In the analysis, it is shown that the proposed observer can estimate measured and unmeasured system parameters satisfactorily under healthy condition with limited output measurements.

The main objective of this research is to develop a reliable scheme capable of detecting and isolating actuator, sensor, and state faults without the use of model reduction. Novelty and contributions of this paper can be summarized as: (a) development of a filter-based fault isolation and location determination for linear DPS by directly utilizing the PDE model of the system rather than approximated ODE models; (b) development of a Luenberger-type fault detection and isolation scheme for nonlinear DPS without requiring any model reduction as opposed to existing methods [14], [15], [16], [17], [18], [19]; (c) development of fault isolability conditions for actuator, sensor and state faults in DPS based on the proposed scheme. Note that previous works of the authors in the same field [20], [21], [22] only target the detection of faults, do not cover nonlinear DPS, and do not include fault isolation or isolability conditions, which are all covered in this paper.

The paper is arranged as follows. First of all, a class of DPS represented by linear parabolic PDE with actuator, sensor and state faults is presented in Section II. A fault isolation scheme is introduced for linear DPS in Section III. Then fault detection and isolation of nonlinear DPS is discussed in

Section IV. Finally, the proposed schemes are demonstrated in simulation in Section V.

II. NOTATION AND LINEAR SYSTEM DESCRIPTION

Before introducing the system description, the notation is briefly introduced [24]. A scalar function $v_1(x) \in L_2(0,1)$ implies it is square integrable on the Hilbert space $L_2(0,1)$ with its corresponding norm defined by

$$\|v_1\|_2 = \sqrt{\int_0^1 v_1^2(x)dx}. \tag{1}$$

Now consider

$$[L_2(0,1)]^n = \underbrace{L_2(0,1) \times L_2(0,1) \times \ldots \times L_2(0,1)}_{n \text{ times}}, \tag{2}$$

with $v(x,t) = [v_1(x,t), v_2(x,t), \ldots, v_n(x,t)]^T \in [L_2(0,1)]^n$ and the norm of a vector function is defined as

$$\|v\|_{2,n} = \sqrt{\sum_{i=1}^{n} \|v_i\|_2^2} = \sqrt{\int_0^1 v^T(x)v(x)dx}. \tag{3}$$

In addition, $\|\cdot\|$ denotes a Frobenius norm for a matrix or Euclidean norm for a vector. For sake of saving space, a vector, $v(x,t)$ and its partial derivatives are represented as

$$v_t(x,t) = \partial v(x,t)/\partial t, \quad v_x(x,t) = \partial v(x,t)/\partial x, \quad \text{and} \quad v_{xx}(x,t) = \partial^2 v(x,t)/\partial x^2.$$

Now, consider linear DPS expressed by the following parabolic PDE with Dirichlet actuation

$$v_t(x,t) = \varepsilon v_{xx}(x,t) + \Lambda v(x,t) + d(x,t), \tag{4}$$

where $x \in [0,1]$ is the space variable and $t \geq 0$ is the time variable with boundary conditions defined by

$$v_x(0,t) = 0, \quad v(1,t) = U(t), \tag{5}$$

for $x \in (0,1)$ and $t \geq 0$, where $v(x,t) = [v_1(x,t), \ldots, v_n(x,t)]^T \in [L_2(0,1)]^n$ is the state vector of the DPS, $d(x,t)$ is a bounded disturbance vector, $U(t) = [u_1(x,t), \ldots, u_n(x,t)]^T \in \Re^n$ denotes the control input vector, ε is a positive constant, $\Lambda \in \Re^{n\times n}$ is a real valued square matrix, and $y(t) \in \Re^n$ is the system output given by

$$y(t) = v(0,t). \tag{6}$$

A second output will be utilized for location determination of a state fault and it is expressed as

$$y_i(t) = \int_0^1 C(x)v(x)dx, \tag{7}$$

where $C(x) \in \Re^{n\times n}$ being a known function satisfying $\int_0^1 \|C(x)\|^2 dx \leq \bar{c}^2$.

Remark 1: The output defined in (6) is an ideal point sensor and the output given by (7) represents a spatial weighting function of sensors which is a spatial average over the sensed region [25] The output equation (7) is required only for location determination when a state fault is identified. Next, the fault description is defined.

The DPS (4) with a state fault is described as

$$v_t(x,t) = \varepsilon v_{xx}(x,t) + \Lambda v(x,t) + d(x,t) + h_c(y, x_f, x, t), \tag{8}$$

and the boundary conditions with actuator and sensor faults can be written as

$$v_x(0,t) = 0, \quad v(1,t) = U(t) + h_a(t), \tag{9}$$

$$y(t) = v(0,t) + h_s(t). \tag{10}$$

where x_f is the location of a state fault, h_c, h_a and h_s represent state, actuator and sensor fault functions respectively. The fault functions are described by

$$\begin{aligned} h_a(t) &= \Omega(t-t_f)\Phi_a(U(t),t)\,\theta_a, \\ h_s(t) &= \Omega(t-t_f)\Phi_s(t)\theta_s \\ h_c(y, x_f, x, t) &= \Omega(t-t_f)\Phi_c(y,x,t)\,\Delta(x-x_f)\theta_c, \end{aligned} \tag{11}$$

where t_f represents the time when a fault occurs, $\theta_a \in \Re^n$, $\theta_s \in \Re^n$ and $\theta_c \in \Re^n$ are the unknown actuator, sensor and state fault parameter magnitude vector, respectively, with $\Phi_a(U(t),t) = diag(\sigma_i^{(a)}(U(t),t)) \in \Re^{n\times n}$ is an actuator fault basis function, $\Phi_s(t) = diag[\sigma_i^{(s)}(t)] \in \Re^{n\times n}$ denotes a sensor fault basis function, $\Delta(x-x_f) = diag[\delta_i^{(c)}(x-x_f)] \in \Re^{n\times n}$ determines the location of the state fault, and $\Phi_c(t) = diag[\sigma_i^{(c)}(y,x,t)] \in \Re^{n\times n}$ is a state fault basis function.

The term $\Omega(t-t_f) = diag[\Omega_i(t-t_f)], i = 1,2,\ldots n$ represents the time profile of the fault defined by $\Omega_i(\tau) = \begin{cases} 0, & if\ \tau < 0 \\ 1-e^{-\kappa_i \tau}, & if\ \tau \geq 0 \end{cases}$ with constant κ_i denoting the growth rate of the fault. The following standard assumptions are required in order to proceed.

Assumption 1: The disturbance vector is bounded above such that $\|d(x,t)\| \leq \bar{d}$ for all x and $t \geq 0$, where $\bar{d} > 0$ is a known constant. A general form is given in this paper and a more specific representation is found in [15].

Remark 2: The upper bound of the disturbance $\bar{d}$ is required to determine the fault detection threshold.

Assumption 2: The magnitude of the fault parameter vector is considered unknown but assumed to belong to a known compact set Θ_N (i.e. $\theta_N \in \Theta_N \subset \Re^n, N = a,s,c$ where a, s, and c denote actuator, sensor and state faults respectively), Θ_a represents an actuator fault, Θ_s represents a sensor fault and Θ_c stands for a state fault, $\sigma_i^{(N)}$ is a known smooth function with $\sigma_i^{(a)}$ representing an actuator fault, $\sigma_i^{(s)}$ represents a sensor fault and $\sigma_i^{(c)}$ stands for a state fault.

Remark 3: This assumption is needed to assist in selecting isolation thresholds.

Assumption 3: Sensor, actuator or state fault types are considered and only a single fault occurs at a given time.

Assumption 4: For the sake of isolating the actuator, sensor, and state faults, it is assumed that the DPS runs longer than the isolation time t_i.

Assumption 5: The fault functions are considered bounded.

Next a filter-based detection observer is revisited from [20] to monitor the linear DPS and generate the detection residual.

III. FAULT DETECTION AND ISOLATION FOR LINEAR DPS

A fault detection scheme for state fault and isolation framework will be introduced for linear DPS in this section. In order to detect unexpected faults, an observer acting as a model under healthy conditions is utilized to monitor system behavior. A fault causes the residual to increase beyond a detection threshold indicating its presence. Upon detection, a fault isolation scheme is subsequently applied to differentiate the actuator, sensor and state faults. The location will be determined if a fault is identified as a state fault.

A. DETECTION OBSERVER DESIGN

A filter-based observer was designed utilizing an input and a couple of output filters based on an observable form under healthy conditions. The filter-based observer relaxes the need for state vector measurements over the range of space. Next, the detection residual was generated by comparing the estimated outputs from the observer with measured outputs. Since only the output $y(t) = v(0, t)$ is available, the DPS from (4) and (5) is first converted into the observable form by using the transformation [26] given by

$$z(x,t) = v(x,t) - \int_0^x l(x,\tau)\, v(\tau,t)\, d\tau, \tag{12}$$

where $l(x, \tau)$ is the solution to the hyperbolic PDE satisfying $l_{xx} - l_{\tau\tau} = l(x,\tau)\Lambda/\varepsilon$, $l(1,\tau) = 0$ and $l(x,x) = \Lambda(1-x)/(2\varepsilon)$. The following observable form

$$z_t(x,t) = \varepsilon z_{xx}(x,t) + G(x)z(0,t) + d_l(x,t), \tag{13}$$
$$z_x(0,t) = L_0 z(0,t), \quad z(1,t) = U(t), \tag{14}$$
$$y(t) = z(0,t), \tag{15}$$

is obtained where $L_0 = -\Lambda/(2\varepsilon)$, $G(x) = -\varepsilon l_\tau(x,0)$ and $d_l(x,t) = d(x,t) - \int_0^x d(\tau,t) l(x,\tau)\, d\tau$ is bounded since $d(x,t)$ and $l(x,\tau)$ are bounded. Notice $z(0,t)$ is available since $v(0,t) = z(0,t)$. This transformation prevents the unstable term, $\Lambda v(x,t)$, from appearing in the design of filters which are described next.

The system model given by (13) and (14) is a linear PDE with $G(x)z(0,t)$, $L_0 z(0,t)$ and $U(t)$ viewed as external inputs. According to superposition principle, its solution can be expressed by summing the response of the PDE due to each external input [26] considered individually. Therefore, $z(x,t) \in \Re^n$ can be represented by a combination of the solution defined by

$$\Xi_t(x,t) = \varepsilon \Xi_{xx}(x,t), \quad \Xi_x(0,t) = 0, \quad \Xi(1,t) = U(t), \tag{16}$$

where $\Xi(x,t)$ is denoted as an input filter, since it is derived from the input of the actual system $U(t)$ [26].

Then consider

$$A_t(x,t) = \varepsilon A_{xx}(x,t), \quad A_x(0,t) = y(t), \quad A(1,t) = 0, \tag{17}$$

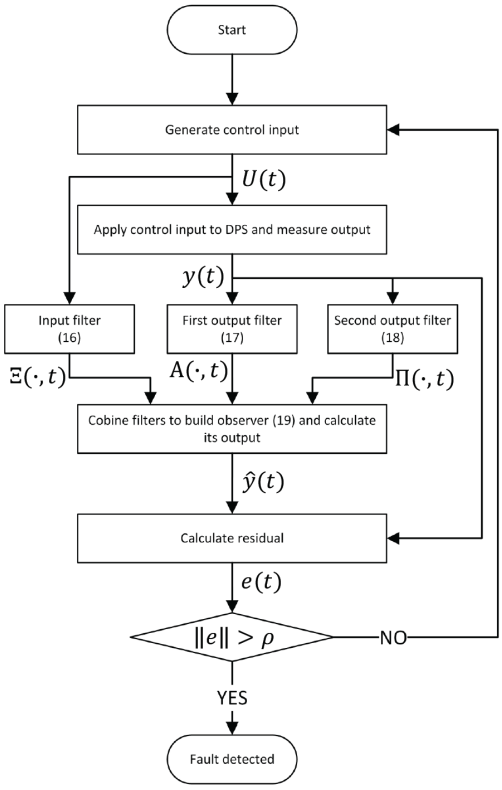

FIGURE 1. Fault detection flowchart.

where $A(x,t)$ is an output filter since it is derived from output of the actual system $y(t)$. It is also important to consider

$$\Pi_t(x,\eta,t) = \varepsilon \Pi_{xx}(x,\eta,t) + \delta(x-\eta)y(t)$$
$$\Pi_x(0,\eta,t) = 0, \quad \Pi(1,\eta,t) = 0, \tag{18}$$

where $\Pi(x,\eta,t)$ is a second output filter. Therefore, the observer with its state, $\hat{z}(x,t) \in \Re^n$, is defined as

$$\hat{z}(x,t) = \Xi(x,t) + L_0 \mathrm{A}(x,t) + \int_0^1 G(s)\Pi(x,s,t)ds. \tag{19}$$

The estimated output and detection residual are given by $\hat{y}(t) = \hat{z}(0,t)$, and $e(t) = y(t) - \hat{y}(t)$. Finally, fault detection is performed by comparing the residual with a predefined threshold. The complete process for fault detection is illustrated in the form of a flowchart in Fig 1.

The dynamics of the observer error $\tilde{z}(x,t) \in \Re^n = z(x,t) - \hat{z}(x,t)$ under healthy condition satisfies

$$\tilde{z}_t(x,t) = \varepsilon \tilde{z}_{xx}(x,t) + d_l(x,t),$$
$$\tilde{z}_x(0,t) = 0, \quad \tilde{z}(1,t) = 0. \tag{20}$$

The detectability condition for the state fault is given next while the fault detection framework, and detectability condition for actuator and sensor faults are reported in [20]. In the presence of a state fault, the system dynamics are modified as (8) with boundary conditions given by (5). Take the partial derivative of the transformation (12) with respect

to t as

$$z_t(x,t) = v_t(x,t) - \int_0^x l(x,\tau)\, v_t(\tau,t)\, d\tau$$

Substitute the dynamics given by (8) to the equation above and apply integration by parts to get

$$\begin{aligned} & z_t(x,t) \\ &= \varepsilon v_{xx}(x,t) - \int_0^x l(x,\tau)\,[\varepsilon v_{\tau\tau}(\tau,t) + \Lambda v(\tau,t)]d\tau \\ &\quad + \lambda v(x,t) + d(x,t) + \int_0^x l(x,\tau)d(\tau,t)d\tau \\ &\quad + h_c(y,x,x_f,t) - \int_0^x l(x,\tau)h_c(y,\tau,x_f,t)d\tau \\ &= \varepsilon v_{xx}(x,t) + \Lambda v(x,t) + \varepsilon l(x,0)\, v_x(0,t) \\ &\quad - \varepsilon l_x(x,x)v(x,t) + \varepsilon l_\tau(x,x)v(x,t) - \varepsilon l_\tau(x,0)v(0,t) \\ &\quad - \varepsilon \int_0^x l_{\tau\tau}(x,\tau)\, v(\tau,t)\, d\tau - \int_0^x l(x,\tau)\,\Lambda v(\tau,t)\, d\tau \\ &\quad + d_l(x,t) + h_c(y,x,x_f,t) - \int_0^x l(x,\tau)h_c(y,\tau,x_f,t)d\tau. \end{aligned} \tag{21}$$

Differentiate the transformation (12) with respect to x to get

$$z_x(x,t) = v_x(x,t) - l(x,x)v(x,t) - \int_0^x l_x(x,\tau)\, v(\tau,t)\, d\tau, \tag{22}$$

$$\begin{aligned} z_{xx}(x,t) = v_{xx}(x,t) - \frac{dl(x,x)}{dx}v(x,t) - l(x,x)v_x(x,t) \\ - l_x(x,x)v(x,t) - \int_0^x l_{xx}(x,\tau)\, v(\tau,t)\, d\tau. \end{aligned} \tag{23}$$

Subtracting $\varepsilon\times$ (23) from (21) and applying the dynamics (8) yields

$$\begin{aligned} & z_t(x,t) - \varepsilon z_{xx}(x,t) \\ &= \left[\Lambda - 2\varepsilon\frac{dl(x,x)}{dx}\right] v(x,t) - \varepsilon l_\tau(x,0)v(0,t) \\ &\quad + d_l(x,t) + h_c(y,x,x_f,t) - \int_0^x l(x,\tau)h_c(y,\tau,x_f,t)d\tau \\ &\quad + \int_0^x [\varepsilon l_{xx}(x,\tau) - \varepsilon l_{\tau\tau}(x,\tau) - l(x,\tau)\,\Lambda]\, v(\tau,t)\, d\tau. \end{aligned}$$

By using the fact that $l_{xx} - l_{\tau\tau} = l(x,\tau)\Lambda/\varepsilon$, $l(1,\tau) = 0$ and $l(x,x) = \Lambda(1-x)/(2\varepsilon)$ we get

$$\begin{aligned} z_t(x,t) = \varepsilon z_{xx}(x,t) + G(x)z(0,t) + d_l(x,t) \\ + h_c(y,x,x_f,t) - \int_0^x l(x,\tau)h_c(y,\tau,x_f,t)d\tau, \end{aligned} \tag{24}$$

with boundary conditions (14) and (15) where $G(x)$ is defined after equation (15). Next, the following theorem will introduce a detectability condition for a state fault by using (24).

Theorem 1 (State Fault Detectability Condition): Consider the observer defined by (19) is utilized to monitor

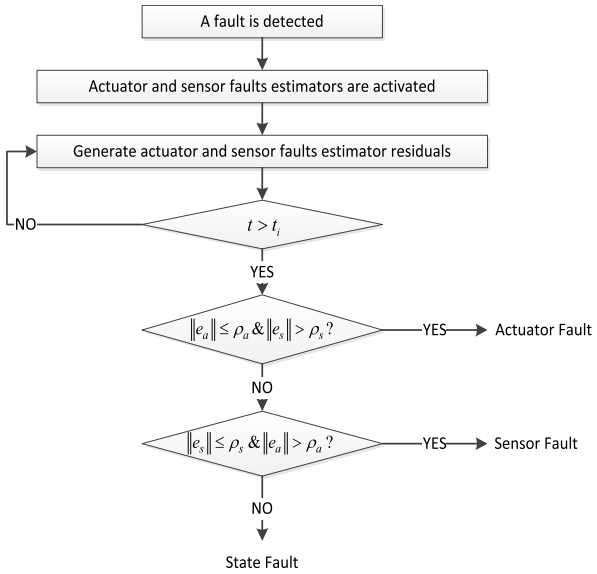

FIGURE 2. Fault isolation scheme.

(24) and (14–15). A state fault initiated at the time instant, t_f, and location, x_f, is detectable if there exists a time $T \ge t_f$ such that for all $t > T$, the following condition

$$\begin{aligned} \Bigg\| \sum_{n=0}^{\infty} \int_{t_f}^{t} \Bigg\{ 2\int_0^1 [h_c(y,x,x_f,\tau) - \int_0^x l(x,\eta)\; h_c(y,\eta,x_f,\tau) \\ \times d\eta]\cos[(n+0.5)\pi x]dx\Bigg\}\, e^{-\varepsilon[(n+0.5)\pi]^2(t-\tau)}d\tau \Bigg\| > 2\rho, \end{aligned} \tag{25}$$

is satisfied where $n = 0, 1, 2, \ldots$ is an integer.

Proof: See Appendix.

Remark 4: The proof shown in the Appendix demonstrates that a state fault satisfying this condition given by (25) can be detectable by using the observer from (19).

The next step is to determine the type and location of the fault.

B. FAULT ISOLATION SCHEME

Upon detecting a fault, the fault type must be identified followed by fault magnitude estimation. In the case of a state fault, the location has to be found.

To determine the fault type, first an additive actuator and sensor fault isolation estimators, to be presented next, are activated as shown in Fig. 2 to generate the corresponding time-varying estimator actuator and sensor output residuals, $e_a(t) = y(t) - y_a(t)$ and $e_s(t) = y(t) - \hat{y}_s(t)$, respectively. The actuator and sensor fault locations are trivial since the locations are automatically determined.

The isolation scheme in Fig 2 shows that when one of the isolation residuals stays below its isolation threshold ρ_a or ρ_s for actuator or sensor respectively (to be defined later in (30) and (37)) and the other exceeds its threshold, the fault is considered to be of that type. A fault is categorized a state fault when both the sensor and actuator isolation residuals

exceed their thresholds. The situation that both of the actuator and sensor isolation residuals keep below their thresholds will not happen due to the assumption that only one type of faults can occur at one time. Next, the actuator and sensor isolation estimators will be introduced.

1) ACTUATOR FAULT ISOLATION ESTIMATOR

Upon detection of a fault, for an additive actuator fault, a fault filter given by

$$F_t(x,t) = \varepsilon F_{xx}(x,t), \quad F_x(0,t) = 0, \tag{26}$$

$$F(1,t) = [\sigma_1^{(a)}(U(t),t), \ldots, \sigma_n^{(a)}(U(t),t)]^T, \tag{27}$$

is incorporated into the observer (19) to construct an actuator fault isolation estimator where $F(x,t) \in \Re^n$ is utilized to estimate the fault function with initial condition $F(x,t_d) = 0$. To match the dimension of $\Phi_a(U(t),t) \in \Re^{n\times n}$, $F_a(x,t) = diag[F(x,t)]$ is used to estimate the fault function. The next theorem will cover the performance of an actuator isolation estimator.

Remark 5: By representing $\Phi_a(U(t),t)$ in (27) as a diagonal matrix to derive the actuator fault filter, the number of PDE equations can be reduced from $n \times n$ to n. In addition, if $[\sigma_1^{(a)}(U(t),t), \ldots, \sigma_n^{(a)}(U(t),t)]^T = U(t)$, the fault filter given by (26) and (27) will be same as the input filter described by (16).

Theorem 2 (Actuator Fault Isolation Estimator Performance): Once detecting a fault at time t_d, consider

$$\hat{z}_a(x,t) = \hat{z}(x,t) + F_a(x,t)\hat{\theta}_a(t), \quad \hat{y}_a(t) = \hat{z}_a(0,t), \tag{28}$$

as the estimator at $t \geq t_d$ for the state and output of the system in the presence of a bounded actuator fault, where $\hat{z}(x,t)$ is given by (19), and $\hat{\theta}_a(t) \in \Re^n$ is the estimated actuator fault parameter vector. Consider the projection algorithm given by

$$\dot{\hat{\theta}}_a(t) = \mathcal{P}_{\Theta_a}\{\beta F_a(0,t)e(t)\}, \tag{29}$$

to tune the parameter vector where $\beta > 0$ is the adaptation rate and $\mathcal{P}_{\Theta_a}\{\cdot\}$ is the projection operator. The actuator output isolation residual, $e_a(t)$, will remain bounded and stays within an fault isolation threshold ρ_a.

Proof: See Appendix.

Remark 6: By defining the actuator fault isolation threshold ρ_a as

$$\rho_a(t) = \rho + \kappa_a(t)\,\|F_a(0,t)\| + \bar{D}, \tag{30}$$

it can be shown in the Appendix that $\|e_a(t)\| \leq \rho_a(t)$ by using estimator defined by (28) with parameter vector tuned by (29). This ensures that an actuator fault can be isolated.

Similarly, a sensor fault isolation estimator will be proposed next.

2) SENSOR FAULT ISOLATION ESTIMATOR

The presence of a sensor fault changes the value of $y(t)$ and thus causes the dynamics of two output filters given by (17) and (18) to provide inaccurate state estimates. Two fault filters are needed in order to mitigate the changes. Upon detecting the fault, consider

$$F_{1t}(x,t) = \varepsilon F_{1xx}(x,t), \quad F_{1x}(0) = [\sigma_1^{(s)}, \ldots, \sigma_n^{(s)}]^T,$$
$$F_1(1,t) = 0, \tag{31}$$

$$F_{2t}(x,\eta,t) = \varepsilon F_{2xx}(x,\eta,t) + \delta(x-\eta)[\sigma_1, \ldots, \sigma_n(t)]^T, \tag{32}$$

$$F_{2x}(0,\eta,t) = 0, \quad F_2(1,\eta,t) = 0, \tag{33}$$

where $F_1(x,t)$ and $F_2(x,t) \in \Re^n$ are states of fault filters. Then the following theorem will establish a sensor fault isolation estimator and define its performance based on these fault filters given by equations above.

Theorem 3 (Sensor Fault Isolation Estimator Performance): Upon detecting a fault, consider the sensor fault isolation estimator for $t \geq t_d$ given by

$$\hat{z}_s(x,t) = \hat{z}(x,t) - [L_0 M(x,t) + \int_0^1 G(s)\Psi(x,s,t)ds]\hat{\theta}_s(t), \tag{34}$$

with

$$\hat{y}_s(t) = \hat{z}_s(0,t) + \Phi_s(t)\hat{\theta}_s(t), \tag{35}$$

to estimate the state and output of DPS, where $\mathrm{M}(x,t) = diag(F_1(x,t))$, $\Psi(x,s,t) = diag(F_2(x,s,t))$ and $\hat{\theta}_s(t) \in \Re^n$ represent the estimated sensor fault parameter vector. Consider the parameter tuning law given by

$$\dot{\hat{\theta}}_s(t) = \mathcal{P}_{\Theta_s}\{\beta F_s^T(0,t)e(t)\}, \tag{36}$$

where $F_s(0,t) = \Phi_s(t) - [L_0\mathrm{M}(0,t) + \int_0^1 G(s)\Psi(0,s,t)ds]$, L_0 is defined after the equation (15) and $\beta > 0$ is the adaptation rate. Then for $t > t_d$, the sensor fault estimator output isolation residual, $e_s(t)$, will be bounded and remains below a predefined sensor fault isolation threshold ρ_s.

Proof: Refer to Appendix.

Remark 7: Define the sensor fault isolation threshold as

$$\rho_s(t) = \rho + \kappa_s(t)\,\|F_s(0,t)\| + \bar{D}. \tag{37}$$

By utilizing the sensor fault estimator given by (34) and output defined by (35) along with the parameter tuned by (36), we can show $\|e_s(t)\| \leq \rho_s(t)$ in the Appendix.

Remark 8: It is shown that in the presence of an actuator or sensor fault, the corresponding isolation estimator output residual should be within its corresponding isolation threshold ρ_a or ρ_s, respectively while the other residual exceeds its isolation threshold. To the contrary, when both sensor and actuator fault isolation estimator output residuals exceed their corresponding isolation thresholds, a state fault is considered to have occurred.

Note the difference between the time-varying isolation thresholds ρ_a or ρ_s and the constant detection threshold ρ. The isolation thresholds (30) and (37) are generally higher than the detection threshold. For example, as shown in Fig 3 (a) the magnitude of the actuator estimator output residual $e_a(t)$ will cross the detection threshold ρ and

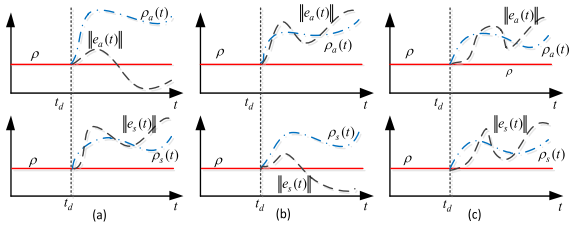

FIGURE 3. Isolation results in the presence of: (a) an actuator fault, (b) a sensor fault, and (c) a state fault.

yet always stay within the isolation threshold of the actuator fault estimator $\rho_a(t)$ in the presence of an actuator fault.

The identification of a state fault requires location determination, which is introduced next.

3) LOCATION DETERMINATION OF A STATE FAULT

First, several state fault filters $i = 1, 2, 3, \ldots, p$, will be designed next with p representing the number of filters, divide the system space $x \in (0, 1)$ into $p + 1$ identical segments, to construct the state fault estimator. By comparing the estimated isolation outputs given by estimators with that of the measured output, p isolation estimator errors will be generated. The estimator generating the minimum error magnitude is believed to be closest to the actual state fault position. Notice that placing more estimators, p, will result in the determination of accurate fault location but this will increase the computational cost.

After introducing the state fault filters and the estimator, the performance of the estimator will be demonstrated and the isolability condition which defines the class of isolable faults will be given. Next, the state fault filters will be introduced.

The system dynamics with a state fault can be written as

$$z_t(x,t) = \varepsilon z_{xx}(x,t) + G(x)z(0,t) + \bar{\Phi}_c(y,x,x_f,t)\theta_c + d_l(v,x,t), \quad (38)$$

with boundary conditions given by (14) and (15) where

$$\bar{\Phi}_c(y,x,x_f,t) = \Phi_c(y,x,t)\Delta(x-x_f) - \int_0^x l(x,\tau)\,\Phi_c(y,\tau,t)\Delta(\tau-x_f)d\tau. \quad (39)$$

In order to construct the state fault isolation estimators, fault filters are incorporated into the observer (19). The state of the estimator, $\hat{z}^{(i)}(x,t)$ at location $x = x_i$ with corresponding estimated output $\hat{y}^{(i)}(t)$ can be represented as

$$\hat{z}^{(i)}(x,t) = \hat{z}(x,t) + F_c^{(i)}(x,t)\hat{\theta}_c^{(i)}(t), \quad (40)$$

$$\hat{y}^{(i)}(t) = \hat{z}^{(i)}(0,t). \quad (41)$$

where $F_c^{(i)}(x,t)$ represents i^{th} fault filter at position $x = x_i$ for $x_i \in (0,1)$ with $i = 1, \ldots p$. The fault filter is designed using

$$\partial F_c^{(i)}(x,t)/\partial t = \varepsilon \partial^2 F_c^{(i)}(x,t)/\partial x^2 + \bar{\Phi}_c(y,x,x_i,t), \quad (42)$$

$$\partial F_c^{(i)}(0,t)/\partial x = 0, \quad F^{(i)}(1,t) = 0, \quad (43)$$

with

$$\bar{\Phi}_c(y,x,x_i,t) = \Phi_c(y,x,t)\Delta(x-x_i) - \int_0^x l(x,\tau)\,\Phi_c(y,\tau,t)\Delta(\tau-x_i)d\tau$$

where $F_c^{(i)}(x,t) \in \Re^{n\times n}$ is the i^{th} fault filter state, $\hat{\theta}^{(i)}(t)$ is the adaptive parameter vector of i^{th} state fault estimator. The state estimation error is defined as

$$\tilde{z}^{(i)}(x,t) = z(x,t) - \hat{z}^{(i)}(x,t), \quad (44)$$

whereas the output residual is given by $e^{(i)}(t) = y(t) - \hat{y}^{(i)}(t)$. In order to study the performance of the estimation error $\tilde{z}^{(i)}(x,t)$, define

$$\bar{z}^{(i)}(x,t) = \hat{z}(x,t) + F_c^{(i)}(x,t)\theta_c. \quad (45)$$

It can be observed that as $\hat{\theta}_c^{(i)}(t) \to \theta_c$, the estimator state defined by (40) is the same as (45).

Define $\mu^{(i)}(x,t) = z(x,t) - \bar{z}^{(i)}(x,t)$ and its dynamics are given by

$$\mu_t^{(i)}(x,t) = \varepsilon\mu_{xx}^{(i)}(x,t) + d_l(x,t) + [\bar{\Phi}_c(y,x,x_f,t) - \bar{\Phi}_c(y,x,x_i,t)]\theta_c, \quad (46)$$

$$\mu_x^{(i)}(0,t) = 0, \quad \mu^{(i)}(1,t) = 0. \quad (47)$$

From the definition of $\tilde{z}^{(i)}(x,t)$ and $\mu^{(i)}(x,t)$ we can get $\tilde{z}^{(i)}(x,t) = \mu^{(i)}(x,t) + F_c^{(i)}(x,t)\tilde{\theta}_c^{(i)}(t)$. If the estimator is located at the same position as the actual fault, i.e. $x_i = x_f$, $\mu^{(i)}(x,t)$ will have same dynamics as the one given by (20) which is bounded for all $x \in [0,1]$, $t \geq t_d$ and the bound only depends on the upper bound of the disturbance. An adaptive update law is proposed to tune the adaptive parameter and an identifiable condition, which defines the class of state faults whose location can be identified using the proposed estimators, is included in the next theorem.

Theorem 4 (State Fault Estimator Performance): Let the state fault estimator be defined by (40) and (41) with parameter update law be presented as

$$\dot{\hat{\theta}}_c^{(i)}(t) = \beta[F_c^{(i)}(0,t)]^T e^{(i)}(t) - \gamma\hat{\theta}_c^{(i)}(t), \quad (48)$$

where γ is a positive constant and $0 < \beta < (\pi^2 - 4)/2$ is the adaptation rate parameter to be used to estimate the system state described by (38) and (14) upon detecting a state fault. By comparing the actual isolation output defined in (7) with the estimated isolation output defined by

$$\hat{y}_i(t) = \int_0^1 C(x)\hat{v}^{(i)}(x)dx, \quad (49)$$

where $\hat{v}^{(i)}$ is the estimated system state given by $\hat{v}^{(i)}(x,t) = \hat{z}^{(i)}(x,t) + \int_0^x K(x,\tau)\,\hat{z}^{(i)}(\tau,t)\,d\tau$ with $\bar{k} = \|K(x,\tau)\|_{x\in[0,1]}$ and $K(x,\tau)$ being the kennel matrix of the inverse transformation

$$v^{(i)}(x,t) = z^{(i)}(x,t) + \int_0^x K(x,\tau)\,z^{(i)}(\tau,t)\,d\tau, \quad (50)$$

the location of a state fault occurred at position $x = x_f$ is identifiable provided the state fault mismatch function

$\eta_i(x) = \bar{\Phi}_c(y, x, x_f, t) - \bar{\Phi}_c(y, x, x_i, t)$ and fault filters defined by (42) and (43) satisfy

$$\begin{aligned} \|\eta_s\| &> \|\eta_r\| \quad \text{and } \chi_s \int_0^1 \left\| F_c^{(s)}(x,t) \right\| dx \\ &> \chi_r \int_0^1 \left\| F_c^{(r)}(x,t) \right\| dx \quad \text{when } \left| x_s - x_f \right| \\ &> \left| x_r - x_f \right| \quad \text{for } s \text{ and } r \in 1, \ldots p, \end{aligned} \tag{51}$$

where $\chi_i = \sqrt{(\|\eta_i\|^2 + d_l^2)/\varepsilon\gamma + \theta_{c\max}^2}$, $i = r, s$.

Proof: See Appendix.

Remark 9: It is shown in the Appendix that the isolation output residual defined by $\tilde{y}_i^{(i)}(t) = y_i(t) - \hat{y}_i^{(i)}(t)$ is bounded by

$$\begin{aligned} \left\| \tilde{y}_i^{(i)}(t) \right\| \le \bar{c}\sqrt{(2+4\bar{k}^2)}[\sqrt{2\gamma\theta_{c\max}^2 + 2[\|\eta_i\|^2 + d_l^2]/\varepsilon} \\ + \chi_i \int_0^1 \left\| F_c^{(i)}(x,t) \right\| dx], \end{aligned} \tag{52}$$

when (51) holds and it is clear that the less the distance between the actual fault and filter location given by $S_i = \left| x_f - x_i \right|$, the smaller will be the bound given by (52). Therefore, the true fault location is determined as the one that is closest to the state fault estimator generating a residual that is minimum over others.

Remark 10: The identifiable condition defined by (51) has two parts because from the isolation output residual given by (52), we can obtained that the magnitude of the residual is determined by the value of both $\|\eta_i\|$ and $\chi_i \int_0^1 \left\| F_c^{(i)}(x,t) \right\|$.

In order to isolate an actuator, sensor and state fault, an isolable condition is required which will be introduced next.

4) FAULT ISOLABILITY CONDITION

In this part, a fault isolability condition is derived on the basis of the proposed fault isolation scheme to define the class of faults that can be isolated. Faults which can produce enough difference on the measurements are simpler to isolate. For the sake of expressing this difference, define a fault mismatch function

$$h^{rm}(t) \triangleq F_r(0,t)\theta_r - F_m(0,t)\hat{\theta}_m(t), \tag{53}$$

where $r = a, s, c$ and $F_r(0,t)\theta_r$ represents the change of the measured output caused by an actuator fault, sensor fault or state fault respectively, $m = a, s$ and $F_m(0,t)$ denotes effect caused by an estimated actuator fault or sensor fault on the output and $r \neq m$. The fault mismatch function can be viewed as the difference between the actual change of the output $F_r(0,t)\theta_r$ due to the fault and estimated change of the output $F_m(0,t)\theta_m$ given by any other fault estimator m whose framework does not match with the actual fault r.

Theorem 5 (Isolability Condition for Linear DPS): A fault r that has been detected is isolable if for each estimator $m \in \{a, s\}\backslash\{r\}$, there exists a time $t_i > t_d$ such that the fault mismatch function defined by (53) satisfies the following inequality

$$\left\| h^{rm}(t) \right\| > 2\rho + \kappa_m(t) \left\| F_m(0,t) \right\| + \bar{D}. \tag{54}$$

Proof: See Appendix.

Next the fault isolation of nonlinear DPS is introduced.

IV. NONLINEAR SYSTEM DESCRIPTION

A class of DPS represented by a bank of nonlinear PDEs will be introduced in this section. The system description under healthy conditions will be presented first and with actuator and sensor faults will be given in the second part.

A. SYSTEM DESCRIPTION WITHOUT FAULTS

The state representation of a class of nonlinear DPS is expressed as

$$\frac{\partial v(x,t)}{\partial t} = c\frac{\partial^2 v(x,t)}{x^2} + f(v,x) + d(v,x,t), \tag{55}$$

with boundary conditions given by

$$v_x(0,t) = Qv(0,t), \quad v(1,t) = u(t), \tag{56}$$

and

$$y(t) = v(0,t), \quad y_s(t) = v_x(0,t), \quad y_a(t) = v(1,t), \tag{57}$$

where $x \in [0,1]$ is the space variable, $t \ge 0$ is the time variable, $v(x,t) \in \Re^n$ represents the state vector, $y(t)$ is the measured output for observer design and fault detection, $y_s(t)$ is an additional required measurement for sensor fault isolation while $y_a(t)$ is the required measurement for an actuator fault isolation, $f(v,x) \in \Re^n$ is the nonlinear vector function, $d(x,t) \in \Re^n$ denotes the disturbance, $Q \in \Re^{n\times n}$ is a nonzero square matrix, and $c > 0$ is a constant.

Assumption 6: The nonlinear vector function $f(v,x)$ satisfies the following conditions

a. $f(v,x)$ is Lipschit continuous in v, $\mathbb{C}^0$ in x, $\mathbb{C}^1$ in t and v for $x \in [0,1]$, $t \ge 0$ and $v(x) \in L_2(0,1)$.
b. $f(v,x)$ should satisfy

$$f(v+\Delta v, x) - f(v,x) = \frac{\partial f(v,x)}{\partial v}\Delta v + \varepsilon_f(\Delta v, x),$$

where Δv represents a small change in v and $\varepsilon_f(\Delta v, x)$ is the approximation error satisfying $\left\| \varepsilon_f \right\|_{2,n} \le \bar{\varepsilon}_f$.

Remark 11: Assumption 6 (a) indicates that $\frac{\partial f(v,x)}{\partial v}$ is bounded.

Remark 12: In order to meet the requirement $\left\| \varepsilon_f \right\|_{2,n} \le \bar{\varepsilon}_f$ in Assumption 6 (b), Δv needs to be small enough implying that the initial condition of the observer which will be introduced in Section IV-B should be close to the initial condition of the system described by (55) and (56).

In the presence of a state fault, the state representation given by (55) is modified as

$$\frac{\partial v(x,t)}{\partial t} = c\frac{\partial^2 v(x,t)}{x^2} + f(v,x) + d(x,t) + h_c(u,y). \tag{58}$$

Similarly, the boundary conditions are changed as

$$v_x(0,t)=0, \quad v(1,t)=u(t)+h_a(u), \tag{59}$$

in the presence of an actuator fault and

$$y(t)=v(0,t)+h_s(t), \tag{60}$$

in the presence of a sensor fault.

Assumption 7: The fault type considered in the nonlinear system is state, actuator or sensor faults and only one fault occurs at any time.

Next, a detection observer will be first presented and then a fault isolation scheme for differentiating state, actuator and sensor faults will be proposed.

B. OBSERVER DESIGN

First the design of the observer will be introduced. Next for the sake of selecting suitable gains of the observer, the observer error dynamics will be considered. It will be shown that by appropriately selecting observer gains, the error dynamics will be bounded. To monitor the system behavior described by (55), (56) and (57), a detection observer is proposed as

$$\frac{\partial \hat{v}(x,t)}{\partial t}=c\frac{\partial^2 \hat{v}(x,t)}{\partial x^2}+f(\hat{v},x)+P_1(x,t)(y-\hat{y}), \tag{61}$$

$$\frac{\partial \hat{v}(0,t)}{\partial t}=Qy(t)+P_{10}(t)(y-\hat{y}), \quad \hat{v}(1,t)=u(t), \tag{62}$$

$$\hat{y}(t)=\hat{v}(0,t), \tag{63}$$

where $\hat{v}(x,t) \in \Re^n$ represents the observer state, $P_1(x) \in \Re^{n\times n}$ and $P_{10} \in \Re^{n\times n}$ are observer gains and $\hat{y}(t) \in \Re^n$ is the estimated output.

Define detection residual as $e(t) \in \Re^n = y(t)-\hat{y}(t)$, and the observer error is given by $\tilde{v} \in \Re^n = v-\hat{v}$. Then, by applying Assumption 6, the dynamics of the observer error can be obtained as

$$\tilde{v}_t(x,t)=c\tilde{v}_{xx}(x,t)+A(t)\tilde{v}(x,t)+\varepsilon_f(\tilde{v},x) - P_1(x,t)e(t)+d(x,t), \tag{64}$$

subject to the boundary conditions given by

$$\tilde{v}_x(0,t)=-P_{10}(t)e(t), \quad \tilde{v}(1,t)=0, \tag{65}$$

where $A(t)=\frac{f(v,x,t)}{v^T}\Big|_{v=\hat{v}}$. It can be shown that when the observer gains are selected as [23]

$$P_1(x,t)=c\frac{\partial L(x,0,t)}{\partial \tau}, \quad P_{10}(t)=L(0,0,t), \tag{66}$$

then by applying the transformation

$$\tilde{v}(x,t)=\Xi(x,t)-\int_0^x L(x,\tau,t)\,\Xi(\tau,t)\,d\tau, \tag{67}$$

to the observer error dynamics described by (64) and (65), it will be converted into a stable system given by

$$\frac{\partial \Xi(x,t)}{\partial t}=c\frac{\partial^2 \Xi(x,t)}{\partial x^2}-b(t)\Xi(x,t) + \varepsilon_{fM}(\tilde{v},x)+d_M(x,t), \tag{68}$$

$$\frac{\partial \Xi(0,t)}{\partial x}=0, \quad \Xi(1,t)=0. \tag{69}$$

where $L(x,\tau,t)$ is the unique solution to the well-posed PDE [23] given by

$$\frac{\partial L(x,\tau,t)}{\partial t}=A(t)L(x,\tau,t)+b(t)L(x,\tau,t) + c[\frac{\partial^2 L(x,\tau,t)}{\partial \tau^2}-\frac{\partial^2 L(x,\tau,t)}{\partial x^2}], \tag{70}$$

$$L(1,\tau,t)=0, \quad L(x,x,t)=\frac{(x-1)}{2c}[A(t)+b(t)I_{n\times n}], \tag{71}$$

$\Xi(x,t) \in \Re^n$, $L(x,\tau,t) \in \Re^{n\times n}$, and $b(t) \geq 0$ is an arbitrary scalar, $d_M(x,t)=d(x,t)+\int_0^x M(x,\eta,t)d(\eta,t)d\eta$ and $\varepsilon_{fM}(\tilde{v},x) = \varepsilon_f(\tilde{v},x)+\int_0^x M(x,\eta,t)\varepsilon_f(\tilde{v},\eta)d\eta$ with $M(x,\eta,t) \in \Re^{n\times n}$ is the kennel matrix of the inverse transformation given by

$$\Xi(x,t)=\tilde{v}(x,t)+\int_0^x M(x,\eta,t)\,\tilde{v}(\eta,t)\,d\eta. \tag{72}$$

The following theorem shows the performance of the detection observer defined by (61), (62) and (63).

Theorem 6 (Detection Observer Performance): Let the observer defined by (61), (62), and (63) to estimate the unmeasured states and measured output of the DPS given by (55), (56) and (57). In the absence of a fault, detection residual $e(t)$ will be bounded and maintained below a detection threshold ρ. A fault can cause $e(t)$ to increase and exceed the threshold ρ.

Proof: Refer to Appendix.

Remark 13: It is shown in the Appendix that under healthy conditions the detection residual defined as $e(t)=v(0,t)$ is bounded by

$$\|e(t)\| \leq 2\sqrt{\frac{17c^3}{\sqrt{2[c+2b(t)][16b(t)+1]}}}(\bar{d}_M+\bar{\varepsilon}_{fM}),$$

and the bound depends upon the disturbance bound. Based on this bound, a predefined threshold ρ is selected, and in the absence of any fault, the magnitude of the detection residual should be below the threshold. In the presence of any type of fault (Fig. 4), the measured output will deviate from the estimated output and thereby cause the detection residual to increase and exceed the predefined threshold. In that case, a fault is declared to be active.

C. FAULT ISOLATION SCHEME

Once a fault is detected by using the proposed observer as shown in Section III-B, the fault type needs to be identified. In order to isolate these faults, it is assumed that the system operates longer than the isolation time t_i.

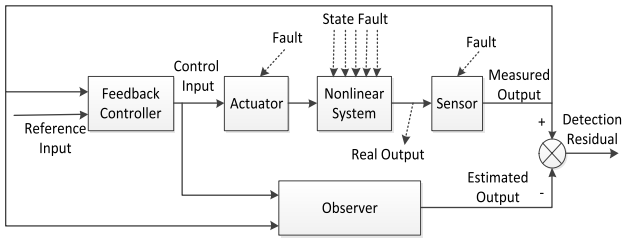

FIGURE 4. Fault detection scheme.

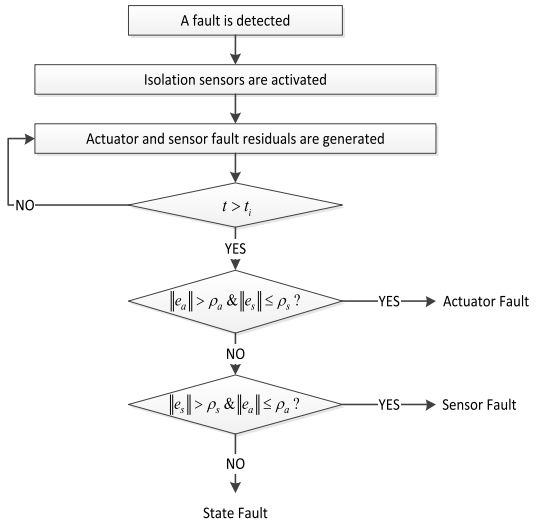

FIGURE 5. Fault isolation scheme.

The isolation scheme given by Fig. 5 indicates that after detecting a fault, by using the measurements defined by (57) and the estimated output given by the observer, the actuator and sensor fault isolation residuals defined by $e_a = y_a(t) - \hat{v}(1, t)$ and $e_s(t) = y_s(t) - Qy(t)$ respectively are generated. Because the presence of an actuator/sensor fault can only cause the corresponding fault isolation residual to increase, if the actuator fault isolation residual e_a exceeds its isolation threshold ρ_a and the other isolation residual keeps below its isolation threshold, an actuator fault will be declared; similar a sensor fault is declared. If neither of the residuals exceeds their corresponding thresholds, the fault is considered as a state fault.

Theorem 7 (Fault Isolability Condition): Upon detecting a fault at $t = t_d$, let the additional measurements y_a and y_s defined by (57) be used to generate actuator and sensor fault isolation residuals defined as $e_a(t) = y_a(t) - \hat{v}(1, t)$ and $e_s(t) = y_s(t) - Qy(t)$. Then

I. An actuator fault will be isolable if there exists a time $t_a > t_d$ such that the magnitude of the actuator fault satisfies $\|h_a(u; t_a)\| > \rho_a$;
II. A sensor fault will be isolable if there exists a time $t_s > t_d$ that the magnitude of the sensor fault satisfies $\|Qh_s(t_s)\| > \rho_s$;
III. A state fault will be identified if $\|e_a(t)\| < \rho_a$ and $\|e_s(t)\| < \rho_s$ for all $t_d < t \le t_i$.

Proof: See Appendix.

Remark 14: Based on the analysis in the Appendix, it is known that either the actuator fault or the sensor fault will cause the fault residual to exceed its corresponding isolation threshold. Therefore, if a fault is detected at t_d and $\|e_a(t)\| < \rho_a$, $\|e_s(t)\| < \rho_s$ for all $t_d < t \le t_i$, a state fault will be considered to occur. The selection of ρ_a and ρ_s can be based on the upper bound of the sensor noise.

V. SIMULATION RESULTS

The proposed fault detection and isolation scheme for linear DPS will be demonstrated in the first part of this section in the simulations by using MATLAB, and the verification of the scheme for nonlinear DPS will be introduced in the second part with a normalized heat equation.

A. FAULT ISOLATION OF A LINEAR SYSTEM

The linear DPS described by linear parabolic PDEs are given by

$$\frac{\partial v(x,t)}{\partial t} = \frac{\partial^2 v(x,t)}{\partial x^2} + \begin{bmatrix} 8 & 1 \\ 2 & 10 \end{bmatrix} v(x,t) + d(x,t), \quad (73)$$

$$\frac{\partial v(0,t)}{\partial x} = [0;0], \quad v(1,t) = u(t), \quad (74)$$

$$y(t) = [y_1(t), y_2(t)]^T = v(0,t), \quad (75)$$

for $x \in [0, 1]$ and $t > 0$ where $v(x, t) \in \Re^{2\times 1}$ represents the system state, $d(x,t) = \begin{bmatrix} 0.05e^{-.5(x-0.2)^2}\sin(t) \\ 0.06e^{-.3(x-0.4)^2}\sin(2t) \end{bmatrix}$ denotes the disturbance, $u(t)$ is the control input implemented at the position $x = 1$, and the output, $y(t)$, is measured at the opposite end.

To simulate the system represented by PDE (73) - (74) and the detection observer using MATLAB, the space and time intervals are selected as $\Delta x = 0.05$ and $\Delta t = 0.01$. Upon detection of a fault, the actuator and sensor fault estimator with outputs given by (28), (34) and (35) are employed to isolate faults. Fig 6 shows that the sensor fault residual stays under its threshold all the time while an actuator fault residual exceeds its threshold. Combining the isolation results with the fault isolation scheme described in Fig 2 indicates a sensor fault. Once a sensor fault is identified, the update law given by (36) will be utilized to estimate fault parameters. After an initial adaptation, as shown in Fig 7(b) and (c), the fault parameter vector can be estimated satisfactorily, which means the detection residual is reduced below the threshold again as shown in Fig 7 (a).

Next, a state fault seeded at $x_f = 0.2$ is considered and the fault function is characterized as

$$h_c(y, x, t) = diag[y_1^2(t), y_2^2(t)]\theta_c(t)\delta(x - 0.2), \quad (76)$$

where $\theta_c(t) = \Omega(t-6)\begin{bmatrix} 1.2 \\ 2.3 \end{bmatrix}$ represents the state fault parameter vector and $\Omega(t-6) = diag(\Omega_i(t-6))$ for

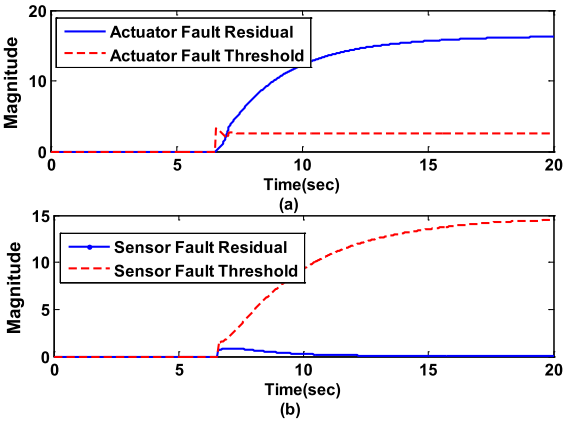

FIGURE 6. Fault isolation of a sensor fault.

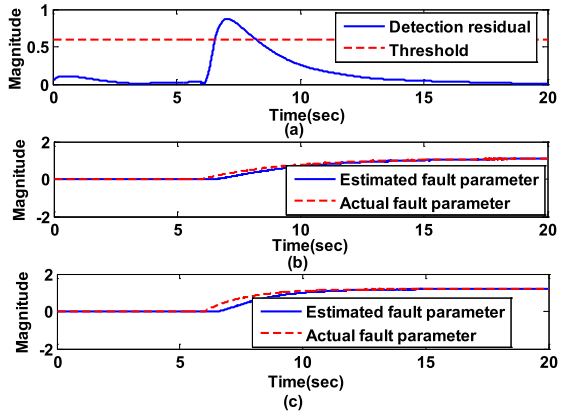

FIGURE 7. Fault detection and estimation results.

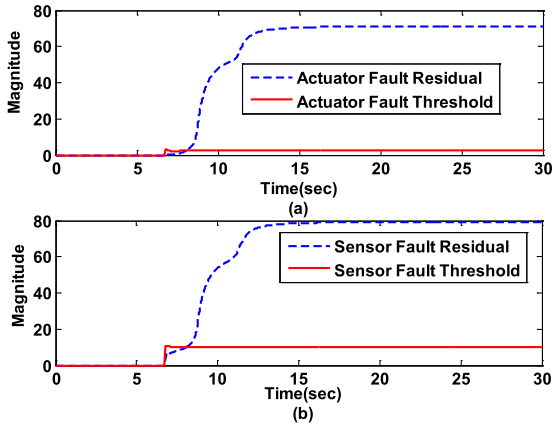

FIGURE 8. Fault isolation of a state fault.

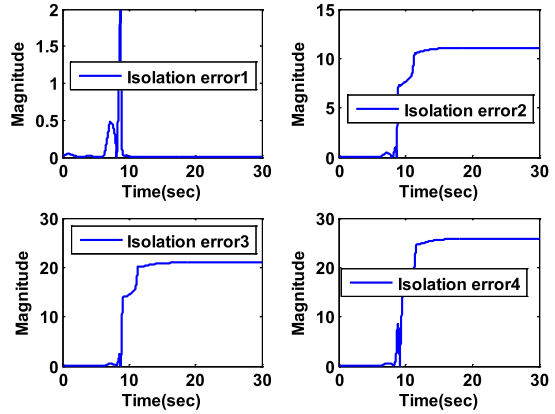

FIGURE 9. Location determination of a state fault.

$i = 1, 2$ which is the time profile of the state fault where $\Omega_i(t-6) = \begin{cases} 0, & if\ t < 6 \\ 1 - e^{-\kappa_i(t-6)}, & if\ t \geq 6 \end{cases}$ with $\kappa_1 = 0.3$ and $\kappa_2 = 0.6$. As noted previously, once a fault is detected, the actuator and sensor fault estimators are utilized to generate the corresponding fault residuals. It is obvious from Fig 8 that both the actuator and sensor fault residuals cross their thresholds implying a state fault.

After the identification of a state fault, the next step is to determine the fault location. In order to achieve this, four fault filters seeded at four different locations $x_i = 0.2, 0.4, 0.6, 0.8$ (see Fig. 9) will be applied with isolation output selected as (notice that the isolation output is not limited to the one defined next)

$$y_i(t) = [v(0.1, t) + v(0.3, t) + v(0.5, t)]/3. \tag{77}$$

Each fault filter can generate an estimated isolation output and using which four isolation residuals are generated by taking the difference between the actual and estimated isolation outputs. The state fault location is determined as $x_f = 0.2$ since Fig 9 shows that the magnitude of the isolation error generated by adding the fault filter at position $x_i = 0.2$ is the minimum.

B. FAULT ISOLATION OF A NONLINEAR SYSTEM

A heat equation with a nonlinear term is expressed as

$$\frac{\partial v(x,t)}{\partial t} = \frac{\partial^2 v(x,t)}{\partial x^2} + 4v(x,t) + 20e^{-\frac{5}{1+v(x,t)}} + d(x,t), \tag{78}$$

subject to the boundary conditions

$$\frac{\partial v(0,t)}{\partial x} = 0.5v(0,t), \quad v(1,t) = u(t), \tag{79}$$

where $v(x, t)$ is the system state, $u(t)$ represents the control input, and $d(x, t) = 0.01\sin(t)e^{-100(x-0.5)^2}$ denotes the disturbance and the measured output for observer design defined as

$$y(0,t) = v(0,t). \tag{80}$$

The observer is developed based on (61)-(63) to monitor system behavior. A fault is declared activated when the detection residual exceeds the detection threshold. Next, the actuator, sensor and state fault are incorporated into the system, respectively, and only one fault is considered at one specific

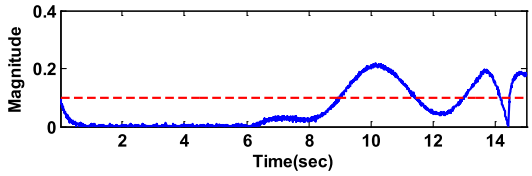

FIGURE 10. Fault detection of an actuator fault.

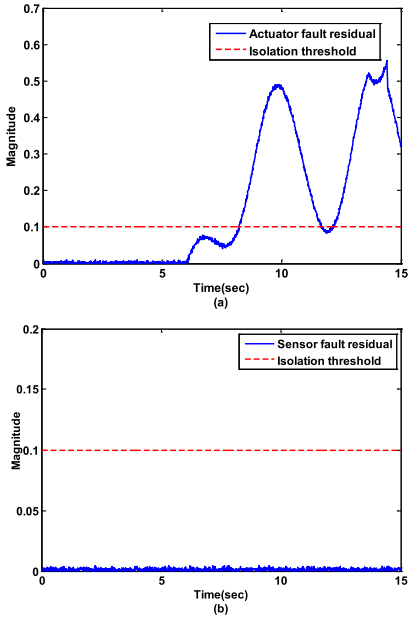

FIGURE 11. Fault isolation results of an actuator fault.

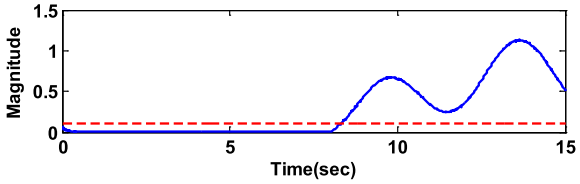

FIGURE 12. Fault detection result of a sensor fault.

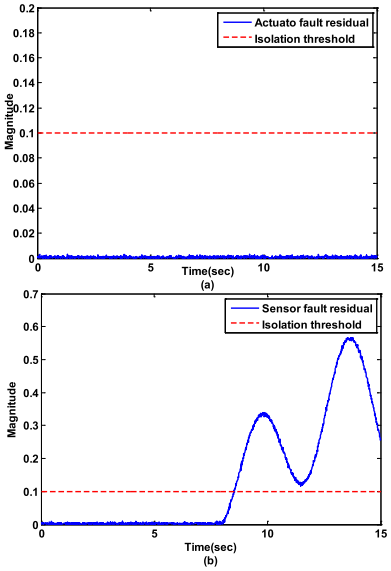

FIGURE 13. Fault isolation results of a sensor fault.

TABLE 1. Performance comparison between the proposed method in this paper and a conventional method from [19].

Method → Performance metric ↓	Proposed PDE-based method	Conventional ODE-based method [19]
TPR	**0.9921**	0.9716
FPR	**0.0130**	0.0529
Average time to detection	2.05 s	**0.98 s**
Percentage of correctly isolated faults	**98.78%**	95.32%
Average time to isolation	5.4 s	**2.13 s**

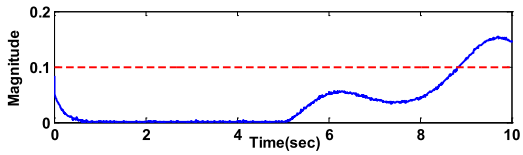

FIGURE 14. Fault detection result of a state fault.

time. The fault functions are expressed as

$$h_a = -0.5(1 - e^{-0.8(t-0.6)})u(t),$$
$$h_s(t) = 1.5(1 - e^{-0.5(t-8)})y_d(t),$$
$$h_c(t) = 0.8(1 - e^{-0.9(t-t_f)})(1 + y(t))^2 e^{-15(x-0.3)^2},$$

where $y_d(t) = 0.3\sin(1.5t) + 0.5$, which is the desired trajectory of the output. To differentiate these three types of faults, two measurements at different locations are utilized which are defined as $y_a(t) = v(1, t)$ and $y_s(t) = v_x(0, t)$.

In the presence of an actuator fault seeded at $t_f = 6s$, it can be observed from Fig. 10 that the fault can be detected within 2.5 s. Fig. 11 shows that only the actuator fault residual exceeded its threshold; thus, an actuator fault is identified. In the case of a sensor fault, it can be seen from Fig 12 and 13 that only the sensor fault isolation residual goes across the threshold indicating a sensor fault.

In the case of state fault, detection occurs around 9 seconds into the simulation as shown in Fig 14. The isolation results as shown in the Fig 15 indicates that neither of the actuator and sensor fault isolation residuals exceed their isolation thresholds so according to the fault isolation scheme of nonlinear DPS, a state fault is identified. Above all, the actuator, sensor, and state faults can be isolated by checking the status of the actuator and sensor fault isolation residuals.

In order to compare the effectiveness of the proposed approach with the existing methods that require model reduction, one of the most recent works in this field was selected [19]. The scheme presented in [19] was slightly modified to fit the system under consideration here. Simulations were performed under identical circumstances using the proposed approach in this paper and the method presented in [19]. Simulations were repeated 100 times with randomized fault locations, magnitudes, rates, and initiation

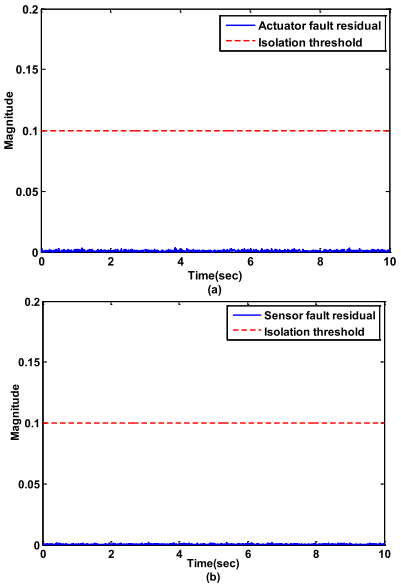

FIGURE 15. Fault isolation results of a state fault.

times. 5 metrics including true positive ratio (TPR), false positive ratio (FPR), average time to detection, percentage of correctly isolated faults, and average time to isolation were selected to evaluate the performance of the methods. Note that in calculation of the average time to detection/isolation, only cases where faults are correctly detected/isolated were included. The results are summarized in Table 1. As expected, the proposed method clearly outperforms the conventional ODE-based method in terms of TPR, FPR, and percentage of correctly isolated faults, which is due to the fact that the proposed method is directly based on the PDE model of the system and thus is more accurate. On the other hand, the conventional method appears to be faster in detecting and isolating of faults. The longer detection time could be due to the conservative selection of detection threshold in this paper, which can be revisited in a future work by employing a time-varying threshold. When the longer time to isolation was investigated, it was found to be rooted mainly in the isolation of state faults. In fact, when it comes to actuator or sensor faults, the average time to isolation of the proposed method is about 0.6 seconds which is well better than the conventional method. The state fault takes longer to be isolated with the proposed method due to the method of isolation that requires a longer wait time to make sure none of the fault residuals are going to exceed their threshold. While this may be a downside, it is possible to alleviate the problem by setting multiple isolation thresholds and monitoring the rate of change of the isolation thresholds after detection. Please note that in the simulations, both methods were implemented at the same sampling rate which was sufficient in this example. However, it must be mentioned that the proposed method has more computational complexity due to the involvement of multiple PDEs that need to be solved in real time and parallel to the actual system without a lag. As a result, the proposed method may require more computational resources compared to conventional methods based on model reduction. This may not be an issue considering the substantial advancement of processing power in the past couple of decades, but still worth mentioning.

VI. CONCLUSION

Fault isolation for DPS is more involved when compared to LPS because the system state in DPS is defined by spatial variations besides temporal variations. The developed actuator and sensor fault estimators for linear DPS with boundary measurement can be utilized to assist in differentiating actuator, sensor and state faults occurring on linear DPS. In addition, the proposed location determination scheme along with the isolation measurement is useful for identifying the location of a state fault provided enough estimators are utilized. To mitigate the lack of fault filters, a Luenberger type observer can be applied to monitor the abnormal behavior of nonlinear DPS. The proposed fault isolation scheme is capable of isolating actuator, sensor, and state faults with additional measurements at boundary conditions to overcome the need for fault filters. The determined fault type and location developed in this research can provide useful information for fault estimation and accommodation. The proposed scheme does have some limitations; (a) it is only suitable for DPS that can be modeled by a parabolic PDE; (b) Although fault detection only requires one boundary measurement, for successful fault isolation three measurements are needed; (c) multiple faults happening at the same time is not supported; (d) more computational power is needed compared to conventional models which must be considered when implementing in real-time on systems with higher dimensions. As future work, the authors plan to address some of these limitations to further enhance the effectiveness and practicality of the proposed scheme.

APPENDIX

Proof of Theorem 1: In the presence of a state fault, the dynamics of the observer error becomes

$$\begin{aligned}\tilde{z}_t(x,t) &= \varepsilon\tilde{z}_{xx}(x,t) + d_l(x,t)\\ &\quad + h_c(y,x,x_f,t) - \int_0^x l(x,\tau)h_c(y,\tau,x_f,t)d\tau,\\ \tilde{z}_x(0,t) &= 0, \quad \tilde{z}(0,t) = 0.\end{aligned}$$

Solving the PDE defined above yields [27]

$$\begin{aligned}&\tilde{z}(x,t)\\ &= \sum_{n=0}^{\infty} e^{-\varepsilon[(n+0.5)\pi]^2(t-t_f)}\tilde{z}_n(t_f)\cos[(n+0.5)\pi x]\\ &\quad + \sum_{n=0}^{\infty}\int_{t_f}^{t} d_m(\tau)e^{-\varepsilon[(n+0.5)\pi]^2(t-\tau)}d\tau\cos[(n+0.5)\pi x]\\ &\quad + \sum_{n=0}^{\infty}\int_{t_f}^{t} e^{-\varepsilon[(n+0.5)\pi]^2(t-\tau)}h_m(\tau)d\tau\cos[(n+0.5)\pi x],\end{aligned}$$

where $\tilde{z}_n(t_f) \in \Re^n$ depends upon the initial condition $e(t_f)$, $d_m(t) = 2\int_0^1 d_l(x,t)\cos[(n+0.5)\pi x]dx$ and $h_m(t) = 2\int_0^1 [h_c(y,x,x_f,t) - \int_0^x l(x,\eta)h_c(y,\eta,x_f,t)d\eta] \times \cos[(n+0.5)\pi x]dx$. The first term in the above equation is the response due to initial condition and the second one is the response due to the fault function and bounded disturbance. By noting detection residual being $e(t) = \tilde{z}(0,t)$, the solution to the detection residual is obtained by substituting $x = 0$ in the above equation as

$$e(t) = \sum_{n=0}^{\infty}\left\{\tilde{z}_n(t_f)e^{-\varepsilon[(n+0.5)\pi]^2(t-t_f)} + \int_{t_f}^{t} d_m(\tau)e^{-\varepsilon[(n+0.5)\pi]^2(t-\tau)}d\tau\right\} + \sum_{n=0}^{\infty}\int_{t_f}^{t} h_m(\tau)e^{-\varepsilon[(n+0.5)\pi]^2(t-\tau)}d\tau.$$

According to triangle inequality ($\|a_1 + a_2\| \geq \|a_2\| - \|a_1\|$) and the equation above we can get

$$\begin{aligned}\|e(t)\| &\geq \left\|\sum_{n=0}^{\infty}\int_{t_f}^{t} h_m(\tau)e^{-\varepsilon[(n+0.5)\pi]^2(t-\tau)}d\tau\right\| \\ &\quad - \left\|\sum_{n=0}^{\infty}\left\{\tilde{z}_n(t_f)e^{-\varepsilon[(n+0.5)\pi]^2(t-t_f)} + \int_{t_f}^{t} d_m(\tau)e^{-\varepsilon[(n+0.5)\pi]^2(t-\tau)}d\tau\right\}\right\| \\ &> 2\rho - \kappa_\rho\left\{\left\|\sum_{n=0}^{\infty}\left\{e^{-\varepsilon[(n+0.5)\pi]^2(t-t_f)}\tilde{z}_n(t_f) + \int_{t_f}^{t} d_m(\tau)e^{-\varepsilon[(n+0.5)\pi]^2(t-\tau)}d\tau\right\}\right\|\right\} \\ &= 2\rho - \rho = \rho,\end{aligned}$$

when (25) holds and the detection threshold is selected as

$$\rho = \kappa_\rho\left\{\left\|\sum_{n=0}^{\infty}\left\{\tilde{z}_n(t_f)e^{-\varepsilon[(n+0.5)\pi]^2(t-t_f)} + \int_{t_f}^{t} d_m(\tau)e^{-\varepsilon[(n+0.5)\pi]^2(t-\tau)}d\tau\right\}\right\|\right\},$$

where $\kappa_\rho > 1$ is a constant, thus assuring the detection of a state fault.

Proof of Theorem 2: The actuator isolation estimator state residual, $\tilde{z}_a(x,t) = z(x,t) - \hat{z}_a(x,t)$, can be written as $\tilde{z}_a(x,t) = \mu(x,t) + F_a(x,t)\theta_a(t)$. Then, the actuator fault estimator output isolation residual can be expressed as

$$e_a(t) = \tilde{z}_a(0,t) = \mu(0,t) + F_a(0,t)\tilde{\theta}_a(t), \tag{81}$$

where $\mu(x,t) = z(x,t) - \bar{z}_a(x,t)$ with $\bar{z}_a(x,t)$ defined as

$$\bar{z}_a(x,t) = \hat{z}(x,t) + F_a(x,t)\theta_a.$$

The equation above is viewed as the ultimate target of $\hat{z}_a(x,t)$ when $\hat{\theta}_a$ is being tuned by (29) and it has the same initial condition as $\hat{z}_a(x,t)$ i.e. $\hat{z}_a(x,t)$ i.e. $\hat{z}_a(t_d) = \bar{z}_a(t_d)$. In the presence of an actuator fault, the system dynamics is described by (13) and (15) with modified boundary conditions given by

$$z_x(0,t) = L_0 z(0,t), \quad z(1,t) = U(t) + \Phi_a(U(t),t)\theta_a. \tag{82}$$

By using the system dynamics given by (13), (15) and (82) and the observer defined by (19), we can obtain the dynamics of $\mu(x,t)$ as

$$\mu_t(x,t) = \varepsilon\mu_{xx}(x,t) + d_l(v,x,t), \quad \mu_x(0,t) = 0, \quad \mu(1,t) = 0, \tag{83}$$

where $d_l(v,x,t)$ is defined after (15). The error dynamics defined in (83) is same as the observer error dynamics given by (20) whose stability has been shown in [20] and [28]. Now to obtain the isolation residual, recall (81), when $t \geq t_d$, and take the norm on both sides to get

$$\|e_a(t)\| \leq \|\mu(0,t)\| + \left\|\tilde{\theta}_a(t)\right\| \|F_a(0,t)\|. \tag{84}$$

By solving the PDE given by (83) and substituting $x = 0$ to the solution we can get for $t \geq t_d$,

$$\mu(0,t) = \sum_{n=0}^{\infty} e^{-\varepsilon[(n+0.5)\pi]^2(t-t_d)}\mu_n(t_d) + \sum_{n=0}^{\infty}\int_{t_d}^{t} d_m(\tau)e^{-\varepsilon[(n+0.5)\pi]^2(t-\tau)}d\tau.$$

Substituting $\|\mu(0,t_d)\| = \|e(0,t_d)\| = \rho$ in the equation above provides

$$\begin{aligned}\|\mu(0,t)\| &\leq \rho + \left\|\sum_{n=0}^{\infty}\int_{t_d}^{t} d_m(\tau)e^{-\varepsilon[(n+0.5)\pi]^2(t-\tau)}d\tau\right\| \\ &= \rho + \bar{D}.\end{aligned}$$

where $\bar{D} = \left\|\sum_{n=0}^{\infty}\int_{t_d}^{t} d_m(\tau)e^{-\varepsilon[(n+0.5)\pi]^2(t-\tau)}d\tau\right\|$. Recalling the inequality given by (84) we can obtain

$$\begin{aligned}\|e_a(t)\| &\leq \|\mu(0,t)\| + \left\|\tilde{\theta}_a(t)\right\| \|F_a(0,t)\| \\ &\leq \rho + \bar{D} + \kappa_a(t)\|F_a(0,t)\|,\end{aligned}$$

where $\kappa_a(t) \geq \left\|\tilde{\theta}_a(t)\right\|$ depends upon the geometric properties of the compact set Θ_a. Recall the actuator fault isolation threshold ρ_a defined by (30) to get $\|e_a(t)\| \leq \rho_a(t)$, which completes the proof.

Proof of Theorem 3: The sensor fault estimator output error is expressed as

$$\begin{aligned}e_s(t) &= y(t) - \hat{y}_s(t) \\ &= \tilde{z}_s(0,t) + \Phi_s(t)\tilde{\theta}_s(t) = \mu(0,t) + F_s(0,t)\tilde{\theta}_s(t),\end{aligned} \tag{85}$$

where $\tilde{z}_s(x,t) = z(x,t) - \hat{z}_s(x,t)$ is the sensor fault isolation estimator state residual, $\mu(x,t) = z(x,t) - \bar{z}_s(x,t)$ with $\bar{z}(x,t)$ is defined as

$$\bar{z}_s(x,t) = \hat{z}(x,t) - [L_0\mathrm{M}(x,t) + \int_0^1 G(s)\Psi(x,s,t)ds]\theta_s,$$

which is viewed as the ultimate target of $\hat{z}_s(x,t)$ when $\hat{\theta}_s$ is being tuned by (36) and has the same initial condition as $\hat{z}_s(x,t)$. In the presence of a sensor fault, the system dynamics becomes (13) and (14) with output expressed as

$$y(t) = z(0,t) + \Phi_s(t)\theta_s,$$

By taking partial derivative of $\mu(x,t)$ with respective to t and x, we can get that the dynamics of $\mu(x,t)$ satisfying (83) indicating the stability of $\mu(x,t)$. Thus, for $t > t_d$ taking the norm on both sides of (85) we can obtain

$$\begin{aligned}\|e_s(t)\| &\leq \|\mu(0,t)\| + \kappa_s \|F_s(0,t)\| \\ &\leq \rho + \kappa_s(t)\|F_s(0,t)\| + \bar{D},\end{aligned}$$

where $\|\mu(0,t)\| \leq \rho + \bar{D}$ for $t > t_d$ and $\kappa_s(t) \geq \left\|\theta_s - \hat{\theta}_s(t)\right\|$ relies on the geometric properties of the compact set Θ_s and $\bar{D}$ is decided by disturbance or uncertainty bound. Substitute the sensor fault isolation threshold defined by (37) to the inequality above yielding $\|e_s(t)\| \leq \rho_s(t)$, which completes the proof.

Proof of Theorem 4: Define a Lyapunov function candidate

$$V = \int_0^1 [\mu^{(i)}(x,t)]^T \mu^{(i)}(x,t)dx/2 + (\tilde{\theta}_c^{(i)})^T \tilde{\theta}_c^{(i)}/2,$$

the derivative of this Lyapunov function with respect to time is given by $\dot{V} = \int_0^1 [\mu^{(i)}(x,t)]^T \frac{\partial \mu^{(i)}(x,t)}{\partial t} dx + [\tilde{\theta}_c^{(i)}]^T \dot{\tilde{\theta}}_c^{(c)}$. By substituting (48) to get

$$\begin{aligned}\dot{V} &= \varepsilon \int_0^1 [\mu^{(i)}(x,t)]^T \mu_{xx}^{(i)}(x,t)dx \\ &+ \int_0^1 [\mu^{(i)}(x,t)]^T d_l(x,t)dx \\ &+ \int_0^1 [\mu^{(i)}(x,t)]^T [\bar{\Phi}_c(y,x,x_f,t) - \bar{\Phi}_c(y,x,x_i,t)]\theta_c dx \\ &+ [\tilde{\theta}_c^{(i)}]^T \dot{\tilde{\theta}}_c^{(i)},\end{aligned}$$

By using integration by parts and Poincare inequality [29] $\left\|\mu^{(i)}\right\|_{2,n}^2 \leq \frac{4}{\pi^2}\left\|\mu_x^{(i)}\right\|_{2,n}^2$ and using the adaptive update law (48), we obtain

$$\begin{aligned}\dot{V} &\leq -\frac{\varepsilon\pi^2}{4}\int_0^1 [\mu^{(i)}(x,t)]^T \mu^{(i)}(x,t)dx \\ &+ \int_0^1 [\mu^{(i)}(x,t)]^T d_l(x,t)dx \\ &+ \int_0^1 [\mu^{(i)}(x,t)]^T [\bar{\Phi}_c(y,x,x_f,t) - \bar{\Phi}_c(y,x,x_i,t)]\theta_c dx \\ &- \beta[\tilde{\theta}_c^{(i)}]^T [F_c^{(i)}(0,t)]^T e^{(i)}(t) + \gamma[\tilde{\theta}_c^{(i)}]^T \hat{\theta}_c^{(i)}.\end{aligned}$$

Because $e^{(i)}(t) = \tilde{z}^{(i)}(0,t) = \mu^{(i)}(0,t) + F_c^{(i)}(0,t)\tilde{\theta}_c^{(i)}(t)$ the above inequality can be rewritten as

$$\begin{aligned}\dot{V} &= -\varepsilon\pi^2 \int_0^1 [\mu^{(i)}(x,t)]^T \mu^{(i)}(x,t)dx/4 \\ &+ \int_0^1 [\mu^{(i)}(x,t)]^T d_l(x,t)dx + \int_0^1 [\mu^{(i)}(x,t)]^T \eta_i(x)dx \\ &- \beta[e^{(i)}(t) - \mu^{(i)}(0,t)]^T e^{(i)}(t) + \gamma[\tilde{\theta}_c^{(i)}]^T \hat{\theta}_c^{(i)} \\ &\leq -\varepsilon\pi^2 \int_0^1 [\mu^{(i)}(x,t)]^T \mu^{(i)}(x,t)dx/4 \\ &+ \int_0^1 [\mu^{(i)}(x,t)]^T d_l(x,t)dx + \int_0^1 [\mu^{(i)}(x,t)]^T \eta_i(x)dx \\ &- \beta[e^{(i)}(t)]^T e^{(i)}(t)/2 + \beta[\mu^{(i)}(0,t)]^T \mu^{(i)}(0,t)/2 \\ &- \gamma[\tilde{\theta}_c^{(i)}]^T \tilde{\theta}_c^{(i)}/2 + \gamma\theta_{c\max}^2/2 \\ &\leq -[\frac{\varepsilon\pi^2}{4} - \frac{\varepsilon(\beta+2)}{2}]\int_0^1 [\mu^{(i)}(x,t)]^T \mu^{(i)}(x,t)dx \\ &- \gamma[\tilde{\theta}_c^{(i)}]^T \tilde{\theta}_c^{(i)}/2 + \gamma\theta_{c\max}^2/2 + (\bar{d}_l^2 + \|\eta_i\|^2)/2\varepsilon\end{aligned}$$

where $\theta_{c\max} \geq \|\theta_c\|$. Therefore, the derivative of Lyapunov function will be less than zero if

$$\begin{aligned}\left\|\mu^{(i)}\right\| &> \sqrt{2\gamma\theta_{c\max}^2 + \frac{2[\|\eta_i\|^2 + d_l^2]}{\varepsilon}} \quad \text{or} \\ \left\|\tilde{\theta}_c^{(i)}\right\| &> \sqrt{\frac{\|\eta_i\|^2 + d_l^2}{\varepsilon\gamma} + \theta_{c\max}^2}.\end{aligned} \tag{86}$$

With the bounds given by (86), the bound of isolation output residual defined by $\tilde{y}_i^{(i)}(t) = y_i(t) - \hat{y}_i^{(i)}(t)$ can be obtained as

$$\begin{aligned}&\left\|\tilde{y}_i^{(i)}(t)\right\| \\ &= \left\|y_i(t) - \hat{y}_i^{(i)}(t)\right\| = \left\|\int_0^1 C(x)[v(x) - \hat{v}^{(i)}(x)]dx\right\| \\ &= \left\|\int_0^1 C(x)\tilde{v}^{(i)}(x)dx\right\| \leq \bar{c}\sqrt{(2+4\bar{k}^2)}\left\|\tilde{z}^{(i)}(x)\right\|_{2,n} \\ &\leq \bar{c}\sqrt{(2+4\bar{k}^2)}[\left\|\mu^{(i)}(x)\right\|_{2,n} + \left\|\tilde{\theta}_c^{(i)}\right\|\int_0^1 \left\|F_c^{(i)}(x,t)\right\|dx] \\ &\leq \bar{c}\sqrt{(2+4\bar{k}^2)}[\sqrt{2\gamma\theta_{c\max}^2 + 2[\|\eta_i\|^2 + d_l^2]/\varepsilon} \\ &+ \sqrt{(\|\eta_i\|^2 + d_l^2)/\varepsilon\gamma + \theta_{c\max}^2}\int_0^1 \left\|F_c^{(i)}(x,t)\right\|dx],\end{aligned}$$

where $\tilde{v}^{(i)}(x) = v(x) - \hat{v}^{(i)}(x)$ is the state error. The bound on the magnitude of the isolation output error of the state fault estimator $\tilde{y}_i^{(i)}$ depends upon the value of $\|\eta_i\|$ and $\chi_i \int_0^1 \left\|F_c^{(i)}(x,t)\right\|dx$. Because the mismatch function $\|\eta_i\|$ and $\chi_i \int_0^1 \left\|F_c^{(i)}(x,t)\right\|dx$ varies with the distance between the actual fault and filter location given by $S_i = \left|x_f - x_i\right|$ yielding the magnitude of $\tilde{y}_i^{(i)}$ changes with the distance S_i. When the condition (51) is satisfied, the location of the state fault will be identified by comparing the isolation output residual generated by state fault estimators at different locations. The true fault location is determined as the one that is closest to the state fault estimator generating a residual that is minimum over others.

Proof of Theorem 5: Upon detecting a fault, recalling equations given by (81) and (85) the actuator/sensor fault estimator error satisfies $e_m(t) = \mu(0,t) + h^{rm}(t)$. According to triangle inequality $\|a_1 + a_2\| \geq \|a_2\| - \|a_1\|$ and the equation above we can get $\|e_m(t)\| \geq \|h^{rm}(t)\| - \|\mu(0,t)\|$.

If the (55) is satisfied and recall that $\|\mu(0,t)\| \leq \rho + \bar{D}$, it is clear that

$$\begin{aligned}\|e_m(t)\| &> 2\rho + \kappa_m(t)\|F_m(0,t)\| + D - \|\mu(0,t)\| \\ &\geq \rho + \kappa_m(t)\|F_m(0,t)\| = \rho_m(t)\end{aligned}$$

where ρ_m is the threshold used for fault isolation defined by (30) and (37).

Proof of Theorem 6: Define a Lyapunov function candidate $V(t) = \|\Xi(t)\|^2_{2,n}/2c + \|\Xi_x(t)\|^2_{2,n}/2c$ whose derivative with respective to t is obtained as

$$\begin{aligned}&\dot{V}(t) \\ &= \int_0^1 \Xi^T(x,t)\Xi_t(x,t)dx/c + \int_0^1 \Xi_x^T(x,t)\Xi_{xt}(x,t)dx/c \\ &= \int_0^1 \Xi^T(x,t)\Xi_{xx}(x,t)dx - b(t)\int_0^1 \Xi^T(x,t)\Xi(x,t)dx/c \\ &\quad + \int_0^1 \Xi^T(x,t)[d_M(x,t) + \varepsilon_{fM}(\tilde{v},x)]dx/c \\ &\quad + \int_0^1 \Xi_x^T(x,t)d\,\Xi_t(x,t)/c,\end{aligned}$$

Substitute the dynamics described by (68) and (69) to the equation above to get

$$\begin{aligned}&\dot{V}(t) \\ &\leq -\|\Xi_x(t)\|^2_{2,n} - b(t)\|\Xi(t)\|^2_{2,n}/c \\ &\quad + \int_0^1 \Xi^T(x,t)[d_M(x,t) + \varepsilon_{fM}(\tilde{v},x)]dx/c \\ &\quad - \|\Xi_{xx}(t)\|^2_{2,n} + b(t)\int_0^1 \Xi_{xx}^T(x,t)\Xi(x,t)dx/c \\ &\quad - \int_0^1 \Xi_{xx}^T(x,t)[d_M(x,t) + \varepsilon_{fM}(\tilde{v},x)]dx/c \\ &\leq -b(t)\|\Xi(t)\|^2_{2,n}/c - [c + b(t)]\|\Xi_x(t)\|^2_{2,n}/c \\ &\quad - \|\Xi_{xx}(t)\|^2_{2,n} + \frac{(\bar{d}_M + \bar{\varepsilon}_{fM})}{c} \\ &\quad \times \int_0^1 \left[\sqrt{\Xi^T(x,t)\Xi(x,t)} + \sqrt{\Xi_{xx}^T(x,t)\Xi_{xx}(x,t)}\right]dx \\ &\leq -\frac{1+16b(t)}{16c}\|\Xi(t)\|^2_{2,n} - \frac{c+2b(t)}{2c}\|\Xi_x(t)\|^2_{2,n} \\ &\quad + \frac{17c^2(\bar{d}_M + \bar{\varepsilon}_{fM})^2}{4},\end{aligned}$$

where $\bar{d}_M \geq \|d_M\|$ and $\bar{\varepsilon}_{fM} \geq \|\varepsilon_{fM}\|$. Therefore, $\dot{V}(t) < 0$ if one of the following conditions is satisfied

$$\|\Xi(t)\|_{2,n} > 2(\bar{d}_M + \bar{\varepsilon}_{fM})\sqrt{\frac{17c^3}{16b(t)+1}}, \quad \text{or}$$

$$\|\Xi_x(t)\|_{2,n} > \sqrt{\frac{17c^3}{2[c+2b(t)]}}(\bar{d}_M + \bar{\varepsilon}_{fM}).$$

By Agmon's inequality

$$\max_{x\in[0,1]} \|\Xi(x,t)\|_2^2 \leq 2\|\Xi(t)\|_{2,n}\|\Xi_x(t)\|_{2,n},$$

we can get $\|e(t)\| \leq 2\sqrt{\frac{17c^3}{\sqrt{2[c+2b(t)][16b(t)+1]}}}(\bar{d}_M + \bar{\varepsilon}_{fM})$. Therefore, the detection residual is bounded and based on the bound defined above, a detection threshold ρ can be selected to assure that in the absence of faults the magnitude of the detection residual remains below the threshold. A fault can cause the magnitude of the detection residual to increase and eventually exceed the threshold which leads to detection of the fault.

Proof of Theorem 7: In the presence of an actuator fault, the boundary conditions are modified as (59), and we can get $e_a(t) = h_a(u;t)$ for $t \geq t_f$. If $\|h_a(u;t_a)\| > \rho_a$, then it can be guaranteed that $\|e_a(t_a)\| > \rho_a$ and thus, an actuator fault is isolated. On the hand, the presence of a sensor fault or state fault will not cause $\|e_a(t)\|$ to go across the isolation threshold ρ_a for all $t_d < t \leq t_i$.

In the case of a sensor fault, the sensor fault residual will become as $e_s(t) = Qv(0,t) - Q[v(0,t) + h_s(t)] = -Qh_s(t)$ for $t > t_f$ due to the sensor fault. It is obvious that if $\|Qh_s(t_s)\| > \rho_s$ then $\|e_s(t_s)\| > \rho_s$ and thus a sensor fault is isolated. However, the occurrence of an actuator or state faults will not make the magnitude of the sensor fault residual to exceed its threshold for all $t_d < t \leq t_i$.

REFERENCES

[1] X. Zhang, M. M. Polycarpou, and T. Parisini, "A robust detection and isolation scheme for abrupt and incipient faults in nonlinear systems," *IEEE Trans. Autom. Control*, vol. 47, no. 4, pp. 576–593, Apr. 2002.
[2] R. J. Patton, "Robustness in model-based fault diagnosis: The 1995 situation," *Annu. Rev. Control*, vol. 21, pp. 103–123, Jan. 1997.
[3] H. Ferdowsi and S. Jagannathan, "A unified model-based fault diagnosis scheme for non-linear discrete-time systems with additive and multiplicative faults," *Trans. Inst. Meas. Control*, vol. 35, no. 6, pp. 742–752, Aug. 2013.
[4] C. Edwards, S. K. Spurgeon, and R. J. Patton, "Sliding mode observers for fault detection and isolation," *Automatica*, vol. 36, no. 4, pp. 541–553, Apr. 2000.
[5] R. J. Patton, J. Chen, and C. J. Lopez-Toribio, "Fuzzy observers for nonlinear dynamic systems fault diagnosis," in *Proc. 37th IEEE Conf. Decis. Control*, vol. 1, Dec. 1998, pp. 84–89.
[6] X. Liu, J. Han, H. Zhang, S. Sun, and X. Hu, "Adaptive fault estimation and fault-tolerant control for nonlinear system with unknown nonlinear dynamic," *IEEE Access*, vol. 7, pp. 136720–136728, 2019.
[7] M. A. Eissa, A. Sali, F. A. Ahmad, and R. R. Darwish, "Observer-based fault detection approach using fuzzy adaptive poles placement system with real-time implementation," *IEEE Access*, vol. 9, pp. 83272–83284, 2021.
[8] X.-Z. Jin, W.-W. Che, Z.-G. Wu, and Z. Zhao, "Adaptive consensus and circuital implementation of a class of faulty multiagent systems," *IEEE Trans. Syst., Man, Cybern. Syst.*, vol. 52, no. 1, pp. 226–237, Jan. 2022.
[9] C. Deng and W.-W. Che, "Fault-tolerant fuzzy formation control for a class of nonlinear multiagent systems under directed and switching topology," *IEEE Trans. Syst., Man, Cybern. Syst.*, vol. 51, no. 9, pp. 5456–5465, Sep. 2021.
[10] M. Patan and D. Ucinski, "Optimal activation strategy of discrete scanning sensors for fault detection in distributed-parameter systems," in *Proc. 16th IFAC World Congr.*, Prague, Czech Republic, 2005, pp. 4–8.
[11] S. Omatu and J. H. Seinfeld, *Distributed Parameter Systems: Theory and Applications*. Oxford, U.K.: Clarendon Press, 1989.
[12] P. D. Christofides, *Nonlinear and Robust Control of PDE Systems: Methods and Applications to Transport-Reaction Processes*. Boston, MA, USA: Birkhaüser, 2001.
[13] A. Friedman, *Partial Differential Equations of Parabolic Type*. Chelmsford, MA, USA: Courier Corporation, 2013.
[14] H. Baruh, "Actuator failure detection in the control of distributed systems," *J. Guid., Control, Dyn.*, vol. 9, no. 2, pp. 181–189, Mar. 1986.

[15] M. A. Demetriou, K. Ito, and R. C. Smith, "Adaptive monitoring and accommodation of nonlinear actuator faults in positive real infinite dimensional systems," *IEEE Trans. Autom. Control*, vol. 52, no. 12, pp. 2332–2338, Dec. 2007.
[16] A. Baniamerian and K. Khorasani, "Fault detection and isolation of dissipative parabolic PDEs: Finite-dimensional geometric approach," in *Proc. Amer. Control Conf. (ACC)*, Jun. 2012, pp. 5894–5899.
[17] G. Rigatos and M. Abbaszadeh, "Fault diagnosis for a PDE suspended-bridge model with Kalman filter and statistical decision making," *IEEE Syst. J.*, vol. 15, no. 2, pp. 2137–2147, Jun. 2021.
[18] J. Zhang, C. Yuan, W. Zeng, P. Stegagno, and C. Wang, "Fault detection of a class of nonlinear uncertain parabolic PDE systems," *IEEE Control Syst. Lett.*, vol. 5, no. 4, pp. 1459–1464, Oct. 2021.
[19] J. Zhang, C. Yuan, W. Zeng, and C. Wang, "Fault detection and isolation of uncertain nonlinear parabolic PDE systems," 2022, *arXiv:2203.15850*.
[20] J. Cai, H. Ferdowsi, and J. Sarangapani, "Model-based fault detection, estimation, and prediction for a class of linear distributed parameter systems," *Automatica*, vol. 66, pp. 122–131, Apr. 2016.
[21] H. Ferdowsi and S. Jagannathan, "Fault diagnosis of distributed parameter systems modeled by linear parabolic partial differential equations with state faults," *J. Dyn. Syst., Meas., Control*, vol. 140, no. 1, Jan. 2018, Art. no. 011010.
[22] H. Ferdowsi, J. Cai, and S. Jagannathan, "Actuator and sensor fault detection and failure prediction for systems with multi-dimensional nonlinear partial differential equations," *Int. J. Control, Autom. Syst.*, vol. 20, no. 3, pp. 789–802, Mar. 2022.
[23] T. Meurer, "On the extended luenberger-type observer for semilinear distributed-parameter systems," *IEEE Trans. Autom. Control*, vol. 58, no. 7, pp. 1732–1743, Jul. 2013.
[24] A. Baccoli, Y. Orlov, and A. Pisano, "On the boundary control of coupled reaction-diffusion equations having the same diffusivity parameters," in *Proc. IEEE Conf. Decision Control (CDC)*, Los Angeles, CA, USA, Dec. 2014, pp. 5222–5228.
[25] Y. Sakawa, "Observability and related problems for partial differential equations of parabolic type," *SIAM J. Control*, vol. 13, no. 1, pp. 14–27, Jan. 1975.
[26] M. Krstic and A. Smyshlyaev, *Boundary Control of PDEs: A Course on Backstepping Designs*, vol. 16. Philadelphia, PA, USA: SIAM, 2008.
[27] P. DuChateau and D. Zachmann, *Applied Partial Differential Equations*. Chelmsford, MA, USA: Courier Corporation, 2012.
[28] J. Cai, "Model based fault diagnosis and prognosis of class of linear and nonlinear distributed parameter systems modeled by partial differential equations," Ph.D. dissertation, Dept. Elect. Comput. Eng., Missouri Univ. Sci. Technol., Rolla, MO, USA, 2016.
[29] G. H. Hardy, J. E. Littlewood, and G. Polya, *Inequalities*. Cambridge, U.K.: Cambridge Univ. Press, 1952.

HASAN FERDOWSI (Member, IEEE) received the Ph.D. degree in electrical engineering from the Missouri University of Science and Technology, in December 2013. He is currently an Assistant Professor of electrical engineering with Northern Illinois University (NIU), where he has been a Faculty Member, since 2017. He is also the Director of the Autonomous Robotics and Controls (ARC) Laboratory, NIU. His research interests include fault diagnosis and fault-tolerant control, adaptive control and estimation, distributed systems, autonomous vehicles, and robotics.

JIA CAI received the Ph.D. degree in electrical engineering from the Missouri University of Science and Technology, in 2016. She was an Electrical Engineer with Predictronics Corporation, from 2017 to 2019. She has been a Software Engineer with Microsoft Corporation, since 2019. Her research interests include adaptive control, fault diagnosis and prognosis, and mathematical optimization.

SARANGAPANI JAGANNATHAN (Fellow, IEEE) was the Site Director of the NSF Industry/University Cooperative Research Center on Intelligent Maintenance Systems for 13 years. He is currently a Rutledge-Emerson Distinguished Professor of electrical and computer engineering with the Missouri University of Science and Technology. His research interests include learning and adaptation, neural network control, secure human-cyber-physical systems, prognostics, and autonomous systems/robotics.